Alkyne/Methylene Coupling Reactions at Adjacent Rh/Os Centers: Stepwise Transformations from C_1- through C_4-Bridged Species

James R. Wigginton, Amala Chokshi, Todd W. Graham, Robert McDonald,‡ Michael J. Ferguson,‡ and Martin Cowie*

Department of Chemistry, University of Alberta, Edmonton, Alberta, Canada T6G 2G2

Received July 18, 2005

Reaction of the methylene-bridged complex $[RhOs(CO)_3(\mu\text{-}CH_2)(dppm)_2][CF_3SO_3]$ (dppm = μ-$Ph_2PCH_2PPh_2$) with dimethyl acetylenedicarboxylate or hexafluorobutyne results in alkyne insertion into the Rh−CH_2 bond, yielding $[RhOs(CO)_3(\mu\text{-}\eta^1\text{:}\eta^1\text{-}RC{=}C(R)CH_2)(dppm)_2][CF_3SO_3]$ (R = CO_2Me (**5**), CF_3 (**6**)). Carbonyl removal from each of these species results in a Rh-bound carbonyl being replaced by a triflate ion. Reaction of **5** with diazomethane results in CH_2 insertion into the Rh−C(R) bond with accompanying C−H activation of the original osmium-bound CH_2 group, yielding $[RhOs(CO)_3(\mu\text{-}\eta^1\text{:}\eta^1\text{-}CH_2C(R){=}C(R)CH)(\mu\text{-}H)(dppm)_2][CF_3SO_3]$ (R = CO_2Me). Reaction of the alkyne-bridged species $[RhOs(CO)_3(\mu\text{-}\eta^1\text{:}\eta^1\text{-}RC{=}CR)(dppm)_2][CF_3SO_3]$ (R = CO_2Me) with diazomethane at −78 °C yields $[RhOs(CO)_3(\mu\text{-}\eta^1\text{:}\eta^1\text{-}CH_2C(R){=}CR)(dppm)_2][CF_3SO_3]$ (**12**), which upon warming to ambient temperature, in the absence of diazomethane, undergoes alkyne deinsertion to yield $[RhOs(CO)_3(\eta^2\text{-}RC{\equiv}CR)(\mu\text{-}CH_2)(dppm)_2][CF_3SO_3]$ (**13**). This species and the inserted product (**12**) appear to be in equilibrium, so reaction of **13** with diazomethane proceeds via **12** to give $[RhOs(CO)_3(\eta^1\text{:}\eta^1\text{-}CH_2CH_2C(R){=}CR)(dppm)_2][CF_3SO_2]$ (**14**), in which the hydrocarbyl fragment is chelating to Os and interacting with Rh via an agostic interaction with one of the Os-bound CH_2 hydrogens. Upon standing for weeks, or more rapidly upon refluxing, compound **14** transforms into an isomer (**15**) in which the C_4 unit has migrated from sites on Os adjacent to Rh to sites on Os remote from Rh. An X-ray structure determination of compound **15** as the BF_4^- salt confirms the geometry of this final species. Reaction of the hexafluorobutyne-bridged species $[RhOs(CO)_3(\mu\text{-}\eta^1\text{:}\eta^1\text{-}RC{=}CR)(dppm)_2][CF_3SO_3]$ (R = CF_3) with diazomethane does not give a product analogous to that described for dimethyl acetylenedicarboxylate, but yields the isomer **6**. These carbon−carbon bond forming processes are discussed.

Introduction

Transition-metal alkylidene complexes play an important role in the formation of carbon−carbon bonds.[1] These alkylidene (or carbene) complexes can be classified into two very different classes depending on whether the carbene moiety is terminally bound to a single metal[2] or bridging a pair of metals.[3] Organometallic species containing terminal alkylidenes (M=CRR′) are widely used as catalysts in a wide range of processes including cyclopropanations,[4] olefin metathesis,[5] ring-opening olefin metathesis polymerization,[5] and alkyne polymerization.[6] Bridging alkylidenes, particularly the prototype methylidene, or methylene fragment,[3] have received much less attention, but have been implicated in carbon−carbon chain growth in the Fischer−Tropsch (FT) process.[7] Although less is known about carbon−carbon bond formation involving the bridging methylene group, insertions of olefins,[8] alkynes,[9] and cumulenes[10] into the M−CH_2 bonds of these groups have been reported, yielding a range of interesting hydrocarbyl fragments.

* Corresponding author. E-mail: martin.cowie@ualberta.ca.
‡ X-ray Crystallography Laboratory.

(1) (a) Doyle, M. P. *Comprehensive Organometallic Chemistry II*; Abel, E. W., Stone, F. G. A., Wilkinson, G., Eds.; Elsevier Science Ltd.: Exeter, UK.; 1995; Vol. 12, pp 387, 421. (b) Hegedus, L. S. *Comprehensive Organometallic Chemistry II*; Abel, E. W., Stone, F. G. A., Wilkinson, G., Eds.; Elsevier Science Ltd.: Exeter, UK.; 1995; Vol. 12, p 549. (c) Stille, J. R. *Comprehensive Organometallic* Chemistry II.; Abel, E. W., Stone, F. G. A., Wilkinson, G., Eds.; Elsevier Science Ltd.: Exeter, UK, 1995; Vol. 12, p 577. (d) Collman, J. P.; Hegedus, L. S.; Norton, J. R.; Finke, R. G. In *Principles and Applications of Organotransition Metal Chemistry*; University Science Books: Mill Valley, CA; 1987; Chapter 16.

(2) See for example: (a) Werner, H. *Organometallic* **2005**, *24*, 1036. (b) King, P. J. *Organomet. Chem.* **2002**, *30*, 282. (c) Whittlesey, M. K. *Organomet. Chem.* **2001**, *29*, 350. (d) Gallap, M. A.; Roper, W. R. *Adv. Organomet. Chem.* **1986**, *25*, 121. (e) Bohle, D. S.; Clark, G. R.; Rickard, C. E. F.; Roper, W. R.; Wright, L. J. *J. Organomet. Chem.* **1988**, *358*, 411.

(3) (a) Herrmann, W. A. *Adv. Organomet. Chem.* **1982**, *20*, 159. (b) Puddephatt, R. J. *Polyhedron* **1988**, *7*, 767.

(4) (a) Maas, G. *Chem. Soc. Rev.* **2004**, *33*, 183. (b) Kirmse, W. *Angew. Chem., Int. Ed.* **2003**, *42*, 1088. (c) Brookhart, M.; Studabaker, W. B. *Chem. Rev.* **1987**, *87*, 411.

(5) (a) Ivin, K. J. *Olefin Metathesis*; Academic Press: London, 1983. (b) Grubbs, R. H.; Tumas, W. *Science* **1989**, *243*, 907. (c) Grubbs, R. H. In *Comprehensive Organometallic Chemistry*; Wilkinson, G., Ed.; Pergamon Press Ltd.: New York, 1982; Vol. 8, p 499. (d) Schrock, R. R. *Acc. Chem. Res.* **1990**, *23*, 158. (e) Feldman, J.; Schrock, R. R. *Prog. Inorg. Chem.* **1991**, *39*, 1. (f) Breslow, D. S. *Prog. Polym. Sci.* **1993**, *18*, 1141. (g) Fischmeister, C.; Custarlenas, R.; Bruneau, C.; Dixneuf, P. H. *NATO Science Series II: Math., Phys. Chem.* **2003**, *122*, 23.

(6) (a) Schlund, R.; Schrock, R. R.; Crowe, W. E. *J. Am. Chem. Soc.* **1989**, *111*, 8004. (b) Park, L. Y.; Schrock, R. R.; Stieglitz, S. G.; Crowe, W. E. *Macromolecules* **1991**, *24*, 3489.

10.1021/om058041x CCC: $30.25
Publication on Web 11/12/2005

In an earlier study, aimed at modeling the involvement of different metals in FT chemistry, we reported the facile coupling of up to four methylene groups promoted by a heterobinuclear Rh/Os species,[11] and together with subsequent investigations on related Rh/Ru[12] and Ir/Ru[13] systems, this work has helped elucidate the roles of the different metals in this coupling reaction and has also pointed out some of the unique properties of the Rh/Os combination.[14] In this unique methylene-coupling sequence we have proposed sequential methylene insertions into the Rh−CH_2 bond of bridging C_1, C_2, and C_3 hydrocarbyl units,[11,14] although the C_2- and C_3-bridged intermediates were never observed. In attempts to learn more about the roles of the elusive C_2- and C_3-bridged intermediates in this process we have attempted to model transformations involving these intermediates through the coupling of methylene units with alkynes[15] and cumulenes[10c] as model C_2 fragments. In this study we report our investigations involving the coupling of methylene groups and alkynes to generate C_3- and C_4-bridged fragments on a RhOs core. Two approaches have been pursued involving either alkyne addition to the methylene-bridged complexes $[RhOs(CO)_n(\mu\text{-}CH_2)(dppm)][X]$ (n = 3, 4; X = BF_4, CF_3SO_3)[11] or the reactions of diazomethane with the alkyne-bridged precursors $[RhOs(CO)_3(\mu\text{-}\eta^1\text{:}\eta^1\text{-}RC{=}CR)(dppm)_2][X]$ (R = CO_2Me, CF_3).[16]

Experimental Section

General Comments. All solvents were dried using the appropriate desiccants, distilled before use, and stored under nitrogen. Reactions were performed under an argon atmosphere using standard Schlenk techniques. Rhodium(III) chloride trihydrate was purchased from Johnson Matthey Ltd., and $Os_3(CO)_{12}$ was obtained from Strem. Diazomethane was generated from Diazald, which was purchased from Aldrich, as were dimethyl acetylenedicarboxylate (DMAD), hexafluoro-2-butyne (HFB), and trimethylamine *N*-oxide. The ^{13}C-enriched Diazald was purchased from Cambridge Isotopes, and ^{13}CO was purchased from Isotech, Inc. The complexes $[RhOs(CO)_4(\mu\text{-}CH_2)(dppm)_2][CF_3SO_3]$ (**1**),[11] $[RhOs(CO)_3(\mu\text{-}CH_2)(dppm)_2][CF_3SO_3]$ (**2**),[11] $[RhOs(CO)_3(\mu\text{-}C(CO_2Me){=}C(CO_2Me))(dppm)_2][CF_3SO_3]$ (**3**),[16] and $[RhOs(CO)_3(\mu\text{-}C(CF_3){=}C(CF_3))(dppm)_2][CF_3SO_3]$ (**4**)[16] were prepared by published procedures.

NMR spectra were recorded on a Varian iNova-400 spectrometer operating at 399.8 MHz for ^1H, 161.8 MHz for ^{31}P, and 100.6 MHz for ^{13}C nuclei. Infrared spectra were obtained on either Nicolet Magna 750 or Nicolet Avator 370 DTGS FTIR spectrometers. The elemental analyses were performed by the microanalytical service within the department. Electrospray ionization mass spectra were run on a Micromass ZabSpec spectrometer by the staff in the mass spectrometry service laboratory. In all cases the distribution of isotope peaks for the appropriate parent ion matched the calculated distribution very closely. Spectroscopic data for all compounds are given in Table 1.

Preparation of Compounds. (a) $[RhOs(CO)_3(\mu\text{-}\eta^1\text{:}\eta^1\text{-}C(CO_2Me){=}C(CO_2Me)CH_2)(dppm)_2][CF_3SO_3]$ (5). Method (i). Compound **2** (62.8 mg, 0.0480 mmol) was dissolved in CH_2Cl_2 (5 mL), and excess dimethyl acetylenedicarboxylate (DMAD) (33.6 μL, 0.274 mmol) was added, resulting in an immediate color change from red to yellow. The solution was stirred for 30 min, after which a yellow residue was precipitated by the addition of 15 mL of diethyl ether and 30 mL of pentane, followed by filtration, washing of the solid by ether/pentane, and drying in vacuo (yield 84%). **Method (ii)**. A 4-fold excess of DMAD (18.4 μL, 0.15 mmol) was added to a THF solution (20 mL) of **1** (50 mg, 0.037 mmol) and heated at reflux for 1 h. After cooling to room temperature, precipitation with diethyl ether (100 mL), and filtering, a yellow solid was obtained (yield 92%). Anal. Calcd for $C_{61}H_{52}O_{10}F_3P_4RhOsS$: C, 50.49; H, 3.61. Found: C, 50.12; H, 3.52. MS: *m/z* 1303 ($M^+ - CF_3SO_3$).

(b) $[RhOs(CO)_3(\mu\text{-}\eta^1\text{:}\eta^1\text{-}C(CF_3){=}C(CF_3)CH_2)(dppm)_2][CF_3SO_3]$ (6). Hexafluoro-2-butyne (HFB) was passed through a CH_2Cl_2 solution (10 mL) of compound **2** (118 mg, 0.090 mmol) at a rate of 2 mL/min for 5 min, resulting in a rapid color change from red to yellow. The solution was stirred for 30 min, followed by the precipitation of a yellow solid by the addition of 15 mL of diethyl ether followed by 30 mL of pentane. The solid was filtered and dried under a stream of argon (yield 82%). Anal. Calcd for $C_{59}H_{46}F_9O_6P_4RhOsS$: C, 49.49; H, 3.29. Found: C, 48.89; H, 3.11. MS: *m/z* 1323 ($M^+ - CF_3SO_3$).

(c) $[RhOsCl(CO)_2(\mu\text{-}\eta^1\text{:}\eta^1\text{-}C(CO_2Me){=}C(CO_2Me)CH_2)(dppm)_2]$ (8). CH_2Cl_2 (5 mL) was added to a mixture of **5** (40 mg, 0.025 mmol) and Et_4NCl (4.5 mg, 0.027 mmol), and after stirring for 30 min an orange solid was precipitated through addition of Et_2O (50 mL) and pentane (50 mL). The solid was filtered, washed with ether, and dried in vacuo (yield 92%). HRMS: *m/z* calcd 1310.1073, found 1310.1075.

(d) $[RhOs(CF_3SO_3)(CO)_2(\mu\text{-}\eta^1\text{:}\eta^1\text{-}C(CO_2Me){=}C(CO_2Me)CH_2)(dppm)_2]$ (9). Nitromethane (5 mL) was added to a mixture of **5** (40 mg, 0.025 mmol) and Me_3NO (2.0 mg, 0.027

(7) (a) Fischer, F.; Tropsch, H. *Brennst.-Chem.* **1926**, *7*, 97. (b) Fischer, F.; Tropsch, H. *Chem. Ber.* **1926**, *59*, 830. (c) Brady, R. C.; Pettit, R. *J. Am. Chem. Soc.* **1980**, *102*, 6181. (d) Brady, R. C.; Pettit, R. *J. Am. Chem. Soc.* **1981**, *103*, 1287. (e) Biloen, P.; Sachtler, W. M. H. *Adv. Catal.* **1980**, *30*, 165. (f) Maitlis, P. M.; Long, H. C.; Quyoum, R.; Turner, M. L.; Wang, Z.-Q. *Chem. Commun.* **1996**, 1. (g) Long, H. C.; Turner, M. L.; Fornasiero, P.; Kaspar, J.; Graziani, M.; Maitlis, P. M. *J. Catal*. **1997**, *167*, 172. (h) Dry, M. E. *Appl. Catal. A: Gen.* **1996**, *138*, 319.

(8) (a) Howard, T. R.; Lee, J. B.; Grubbs, R. H. *J. Am. Chem. Soc.* **1980**, *102*, 6876. (b) Lee, J. B.; Gajola, G. J.; Schaefer, W. P.; Howard, T. R.; Ikariya, T.; Straus, D. A.; Grubbs, R. H.; *J. Am. Chem. Soc.* **1981**, *103*, 7358. (c) Motyl, K. M.; Norton, J. R.; Schauer, C. K.; Anderson, O. P. *J. Am. Chem. Soc.* **1982**, *104*, 7325. (d) Sumner, C. E., Jr.; Riley, P. E.; David, R. E.; Pettit, R. *J. Am. Chem. Soc.* **1980**, *102*, 1752. (e) Theopold, K. H.; Bergman, R. G. *J. Am. Chem. Soc.* **1981**, *103*, 2489. (f) Kao, S. C.; Thiel, C. H.; Pettit, R. *Organometallics* **1983**, *2*, 914.

(9) (a) Dyke, A. F.; Knox, S. A. R.; Naish, P. J.; Taylor, G. E. *J. Chem. Soc., Chem. Commun.* **1980**, 803. (b) Gracey, B. P.; Knox, S. A. R.; Macpherson, K. A.; Orpen, A. G.; Stobart, S. R. *J. Chem. Soc., Dalton Trans.* **1985**, 1935. (c) Sumner, C. E.; Collier, J. A.; Pettit, R. *Organometallics* **1982**, *1*, 1350. (d) Akita, M.; Hua, R.; Nakanishi, S.; Tanaka, M.; Moro-oka, Y. *Organometallics* **1987**, *16*, 5572. (e) Adams, P. Q.; Davis, D. L.; Dyke, A. F.; Knox, S. A. R.; Mead, K. A.; Woodward, P. *J. Chem. Soc., Chem. Commun.* **1983**, 222. (f) Colborn, R. E.; Dyke, A. F.; Knox, S. A. R.; Macpherson, K. A.; Orpen, A. G. *J. Organomet. Chem.* **1982**, *239*, C15. (g) Colborn, R. E.; Davies, D. L.; Dyke, A. F.; Knox, S. A. R.; Mead, K. A.; Orpen, A. G.; Guerchais, J. E.; Roue, J. *J. Chem. Soc., Dalton Trans.* **1989**, 1799. (h) Dennett, J. N. L. Ph.D. Thesis, University of Bristol, Bristol, UK, 2000, Chapter 4. (i) Kaneko, Y.; Suzuki, T.; Isobe, K.; Maitlis, P. M. *J. Organomet. Chem.* **1998**, *554*, 155. (j) Navarre, D.; Parlier, A.; Rudler, H.; Daran, J. C. *J. Organomet. Chem.* **1987**, *322*, 103. (k) Levisalles, J.; Rose-Munch, F.; Rudler, H.; Daran, J. C.; Dranzee, Y.; Jeannin, Y. *J. Chem. Soc., Chem. Commun.* **1981**, 152.

(10) (a) Fildes, M. J.; Knox, S. A. R.; Orpen, A. G.; Turner, M. L.; Yates, M. I. *J. Chem. Soc., Chem. Commun.* **1989**, 1680. (b) Chetcuti, M. J.; Fanwick, P. E.; Grant, B. E. *Organometallics* **1991**, *10*, 3003. (c) Chokshi, A.; Rowsell, B. D.; Trepanier, S. J.; Ferguson, M. J.; Cowie, M. *Organometallics* **2004**, *23*, 4759.

(11) (a) Trepanier, S. J.; Sterenberg, B. T.; McDonald, R.; Cowie, M. *J. Am. Chem. Soc.* **1999**, *121*, 2613. (b) Trepanier, S. J.; Dennett, J. N. L.; Sterenberg, B. T.; McDonald, R.; Cowie, M. *J. Am. Chem. Soc.* **2004**, *126*, 8046.

(12) Rowsell, B. D.; Trepanier, S. J.; Lam, R.; McDonald, R.; Cowie, M. *Organometallics* **2002**, *21*, 3228.

(13) Dell'Anna, M. M.; Trepanier, S. J.; McDonald, R.; Cowie, M. *Organometallics* **2001**, *20*, 98.

(14) Cowie, M. *Can. J. Chem.* **2005**, *83*, 1043.

(15) Rowsell, B. D.; McDonald, R.; Ferguson, M. J.; Cowie, M. *Organometallics* **2003**, *22*, 2944.

(16) Hilts, R. W.; Franchuk, R. A.; Cowie, M. *Organometallics*. **1991**, *10*, 304.

Table 1. Spectroscopic Data for the Compounds

compound	IR ν_{CO} (cm^{-1})[a,b]	NMR[d,e] δ ($^{31}P\{^1H\}$)[f]	NMR[d,e] δ (^1H)[g,h]	NMR[d,e] δ ($^{13}C\{^1H\}$)[h,i]
[RhOs(CO)$_3$(μ-η^1:η^1-C(CO$_2$Me)=C(CO$_2$Me)CH$_2$)-(dppm)$_2$][CF$_3$SO$_3$] (**5**)	2035(s), 2013(m), 1947(s), 1702(m)	26.4 (dm, $^1J_{RhP}$ = 113 Hz), −1.6(m)	4.67 (m, 2H, dppm), 3.94 (m, 2H, dppm), 3.17 (s, 3H), 2.71 (s, 3H), 1.68 (t, br, 2H, $^3J_{PH}$ = 10 Hz, CH$_2$)	191.3 (dt, 1C, $^2J_{PC}$ = 12 Hz, $^1J_{RhC}$ = 51 Hz), 183.7 (t, 1C, $^2J_{PC}$ = 6 Hz), 171.4 (t, 1C, $^2J_{PC}$ = 12 Hz), 7.7 (t, 1C, $^2J_{PC}$ = 7 Hz)
[RhOs(CO)$_3$(μ-η^1:η^1-C(CF$_3$)=C(CF$_3$)CH$_2$)-(dppm)$_2$][CF$_3$SO$_3$] (**6**)	2038(s), 2017(m), 1951(s)	25.1 (dm, $^1J_{RhP}$ = 108 Hz), −2.1 (m)	4.21 (m, 2H, dppm), 4.12 (m, 2H, dppm), 2.00 (s, br, 2H, CH$_2$)	190.9 (dt, 1C, $^2J_{PC}$ = 12 Hz, $^1J_{RhC}$ = 50 Hz), 181.8 (t, 1C, $^2J_{PC}$ = 7 Hz), 171.1 (t, 1C, $^2J_{PC}$ = 12 Hz), 6.7 (t, 1C, $^2J_{PC}$ = 7 Hz)
[RhOsCl(CO)$_2$(μ-$\eta^1\eta^1$-C(CO$_2$Me)=(C(CO$_2$Me)CH$_2$)-(dppm)$_2$] (**8**)	2011(s), 1920(s), 1684(m)	27.9 (br), −3.6 (br)[e] 28.9 (dm, 2P, $^1J_{RhP}$ = 127 Hz), 0.1 (m, 1P), −6.7 (m, 1P)[g]	4.41 (br, m, 4H, dppm), 2.89 (s, 3H), 2.88 (s, 3H), 1.03 (t, 2H, $^3J_{PH}$ = 9 Hz)[e] 4.67 (br, m, 1H, dppm), 4.43 (br, s, 1H, dppm), 4.14 (br, s, 1H, dppm), 3.89 (br s, 1H, dppm), 0.73 (br, s, 2H)[g]	
[RhOs(CF$_3$SO$_3$)(CO)$_2$(μ-η^1:η^1-C(CO$_2$Me)=C(CO$_2$Me)CH$_2$)(dppm)$_2$] (**9**)	2010 (s), 1919 (s), 1727(m), 1687 (w)	28.8 (br), −4.6 (br)	4.50 (s, br, 4H, dppm), 3.60 (s, 3H), 1.69 (s, 3H), 1.08 (t, 2H, $^3J_{PH}$ = 9 Hz, $^1J_{CH}$ = 128 Hz, CH$_2$)	181.8 (t, 1C, $^2J_{PC}$ = 5 Hz), 171.5 (t, 1C, $^2J_{PC}$ = 11 Hz), −3.5 (t, 1C, $^2J_{PC}$ = 10 Hz)
[RhOs(CF$_3$SO$_3$)(CO)$_2$(μ-η^1:η^1-C(CF$_3$)=C(CF$_3$)CH$_2$)-(dppm)$_2$] (**10**)	2018(s), 1926(s)	25.8 (br), −5.1 (m)	4.48 (m, 2H, dppm), 3.92 (m, 2H, dppm), 1.63 (m, br, 2H)	182.9 (t, 1C, $^2J_{PC}$ = 4 Hz), 169.3 (t, 1C, $^2J_{PC}$ = 11 Hz), −5.7 (t, 1C, $^2J_{PC}$ = 11 Hz)
[RhOs(CO)$_3$(μ-η^1:η^1-CH$_2$C(CO$_2$Me)=C(CO$_2$Me)CH)-(μ-H)(dppm)$_2$][CF$_3$SO$_3$] (**11**)	2056(m), 2032(s), 1972(m), 1691(w)	24.3 (dm, $^1J_{RhP}$ = 99 Hz), −8.8 (m)	5.29 (dt, 1H, $^2J_{RhH}$ = 2 Hz, $^3J_{PH}$ = 4 Hz, $^1J_{CH}$ = 161 Hz, μ-CH), 5.14 (m, 2H, dppm), 4.32 (m, 2H, dppm), 4.07 (dt, 2H, $^2J_{RhH}$ = 2 Hz, $^3J_{PH}$ = 11 Hz, CH$_2$), 3.92 (s, 3H), 3.05 (s, 3H), −16.6 (m, 1H, $^1J_{RhH}$ = 14 Hz, μ-H)	188.2 (dt, 1C, $^2J_{PC}$ = 12 Hz, $^1J_{RhC}$ = 46 Hz), 185.0 (t, 1C, $^2J_{PC}$ = 11 Hz) 176.7 (t, 1C, $^2J_{PC}$ = 11 Hz), 118.3 (d, 1C, $^2J_{RhC}$ = 16 Hz, μ-CH), 70.3 (d, br, 1C, $^1J_{RhC}$ = 25 Hz, CH$_2$)
[RhOs(CO)$_3$(μ-η^1:η^1-CH$_2$C(CO$_2$Me)=C(CO$_2$Me))-(dppm)$_2$] [CF$_3$SO$_3$] (**12**)[g]	N. A.	19.6 (dm, $^1J_{RhP}$ = 102 Hz), −17.9 (m)[g]	4.82 (t, 2H, CH$_2$, $^3J_{P(Rh)H}$ = 7 Hz, $^1J_{CH}$ = 152 Hz), 4.26 (m, 2H, dppm), 4.08 (m, 2H, dppm), 3.2 (s, br, 6H)[g]	200.4 (dt, 1C, $^1J_{RhC}$ = 49 Hz, $^2J_{PC}$ = 14 Hz), 192.9 (s, br, 1C), 176.6 (t, 1C, $^2J_{PC}$ = 9 Hz), 103.6 (dm, 1C, $^1J_{RhC}$ = 28 Hz)[g]
[RhOs(CO)$_3$(η^2-C(CO$_2$Me)=C(CO$_2$Me))-(μ-CH$_2$)(dppm)$_2$][CF$_3$SO$_3$] (**13**)	2004 (m), 1968 (m, sh), 1957(s), 1697(m)	32.3 (dm, $^1J_{RhP}$ = 113 Hz), 0.6 (m)	4.01 (m, 2H, dppm), 3.89 (m, 2H, dppm), 3.72 (s, 3H), 2.10 (s, 3H), 1.32 (m, 2H, $^3J_{P(Rh)H}$ = 10 Hz, $^2J_{RhH}$ = 3 Hz, $^1J_{CH}$ = 128 Hz, CH$_2$)	190.8 (dt, 1C, $^1J_{RhC}$ = 52 Hz, $^2J_{PC}$ = 12 Hz), 190.7 (m, 1C), 169.6 (m, 1C), 30.6 (dt, 1C, $^1J_{RhC}$ = 18 Hz, $^2J_{P(Rh)C}$ = 8 Hz, CH$_2$)
[RhOs(CO)$_2$(μ-η^1:η^1–CH$_2$CH$_2$C(CO$_2$Me)=C(CO$_2$Me))-(μ-CO)(dppm)$_2$][CF$_3$SO$_3$] (**14**)	2022 (s), 2003 (s), 1870(m), 1691(w)	23.0 (dm, $^1J_{RhP}$ = 104 Hz), −21.3 (m)	4.00 (m, 2H, dppm), 3.89 (m, 2H, dppm), 3.52 (m, br, 2H, $^3J_{HH}$ = 6 Hz, $^1J_{CH}$ = 128 Hz), 3.43 (s, 3H), 3.09 (s, 3H), 0.89 (m, br, 2H, $^2J_{RhH}$ = 4 Hz, $^3J_{HH}$ = 6 Hz, $^1J_{CH}$ = 116 Hz)	193.4 (dm, 1C, $^1J_{RhC}$ = 9 Hz), 186.7 (ddt, 1C, $^2J_{CC}$ = 3 Hz, $^1J_{RhC}$ = 84 Hz, $^2J_{PC}$ = 18 Hz), 176.7 (dt, 1C, $^2J_{CC}$ = 3 Hz, $^2J_{P(Os)C}$ = 8 Hz), 41.80 (d, 1C, $^1J_{CC}$ = 32 Hz), −7.59 (ddt, 1C, $^1J_{CC}$ = 32 Hz, $^1J_{RhC}$ = 4 Hz, $^2J_{PC}$ = 5 Hz)
[RhOs(CO)$_2$(η^1:η^1-CH$_2$CH$_2$C(CO$_2$Me)=C(CO$_2$Me))-(μ-CO)(dppm)$_2$][CF$_3$SO$_3$] (**15**)	2038 (s), 1976 (m), 1872(m), 1699 (m)	26.0 (dm, $^1J_{RhP}$ = 101 Hz), −9.5 (m)	3.78 (m, 2H, dppm), 3.66 (m, 2H, dppm), 3.27 (s, 3H), 3.15 (s, 3H), 1.87 (4H, overlapping)	201.7 (m, 1C), 190.5 (m, 1C), 182.1 (dm, 1C, $^1J_{RhC}$ = 82 Hz), 39.7 (s, 1C, OsCH$_2$*C*H$_2$), 10.2 (t, 1C, $^2J_{PC}$ = 6 Hz, Os*C*H$_2$CH$_2$)

[a] IR abbreviations: s = strong, m = medium, w = weak, sh = shoulder, br = broad. [b] CH_2Cl_2 solutions. [d] NMR abbreviations: s = singlet, d = doublet, t = triplet, m = multiplet, dm = doublet of multiplets, om = overlapping multiplets, br = broad, dt = doublet of triplets. [e] NMR data at 25 °C in CD_2Cl_2 unless otherwise stated. [f] ^{31}P chemical shifts referenced to external 85% H_3PO_4. [g] NMR data collected at −80 °C in CD_2Cl_2. [h] Chemical shifts for the phenyl hydrogens are not given. [i] ^1H and ^{13}C chemical shifts referenced to TMS. [j] $^{13}C\{^1H\}$ NMR performed with ^{13}CO enrichment.

mmol), and after stirring for 20 min a red solid precipitated. The solid was filtered and dried in vacuo (yield 67%). HRMS *m/z* calcd for $C_{59}H_{52}O_6P_4RhOs$ ($M^+ - CF_3SO_3$) 1275.1384, found 1275.1383.

(e) [RhOs(CF_3SO_3)(CO)$_2$(μ-η^1:η^1-C(CF_3)=C(CF_3)CH_2)(dppm)$_2$] (10). Dichloromethane (5 mL) was added to a mixture of **6** (36 mg, 0.025 mmol) and Me_3NO (2 mg, 0.027 mmol), resulting in a rapid color change from yellow to orange. The solution was stirred for 20 min, and then an orange solid was precipitated by the slow addition of 20 mL of diethyl ether, followed by 40 mL of pentane. The solid was filtered and dried under a stream of argon (yield 76%). HRMS: *m/z* calcd for $C_{57}H_{46}O_2F_6P_4RhOs$ ($M^+ - CF_3SO_3$) 1295.1022, found 1295.1024.

(f) [RhOs(CO)$_3$(μ-η^1:η^1-CH_2C(CO_2Me)=C(CO_2Me)CH)(μ-H)(dppm)$_2$][CF_3SO_3] (11). Diazomethane, generated from 50 mg of Diazald (0.23 mmol, 16 equiv), was vigorously passed through a CH_2Cl_2 solution (10 mL) of compound **5** (50 mg, 0.014 mmol), resulting in a color change from yellow to orange. The orange residue was precipitated using 15 mL of diethyl ether and 30 mL of pentane, then filtered and dried under a stream of argon (yield 86%). HRMS: *m/z* calcd for $C_{61}H_{54}O_7P_4RhOs$ ($M^+ - CF_3SO_3$) 1317.1490, found 1317.1500.

(g) Attempted Reaction of 6 + CH_2N_2. An excess of diazomethane (20 mg, 0.094 mmol, 7 equiv) was passed through an NMR tube containing compound **6** (20 mg, 0.014 mmol) in 0.7 mL of CD_2Cl_2. The color of the solution changed from yellow to orange over the course of 1 day, but only compound **6** was detected via $^{31}P\{^1H\}$ NMR spectroscopy.

(h) [RhOs(CO)$_3$(μ-η^1:η^1-CH_2C(CO_2Me)=C(CO_2Me))(dppm)$_2$][CF_3SO_3] (12). Compound **3** (50 mg, 0.035 mmol) was dissolved in CH_2Cl_2 (15 mL) and cooled to −78 °C. An excess of diazomethane, generated from Diazald (50 mg, 0.23 mmol, 7 equiv), was passed through the solution, resulting in a rapid color change from orange to green. All attempts to isolate **12** by removal of excess diazomethane, thereby preventing further reaction yielding **14** (vide infra), were unsuccessful. Even in the absence of diazomethane compound **12** was unstable, converting into compound **13** upon warming to ambient temperature. Due to this conversion of **12** to **13**, characterization of the former was possible only by NMR spectroscopy.

(i)[RhOs(CO)$_3$(η^2-(CO_2Me)CC(CO_2Me))(μ-CH_2)(dppm)$_2$][CF_3SO_3] (13). Compound **12** was prepared as described in part (h) at −78 °C, and the solution was stirred at this temperature for 30 min. The excess diazomethane was removed by placing the sample under vacuum for 30 min at −78 °C. Then the sample was gradually warmed to room temperature while under dynamic vacuum. As the solution warmed to ambient temperature, its color changed from green to orange. An orange solid was isolated at ambient temperature by the slow addition of 15 mL of diethyl ether followed by 30 mL of pentane. This solid was filtered and then dried under a stream of argon (yield 72%). HRMS: *m/z* calcd for $C_{60}H_{52}O_7P_4RhOs$ ($M^+ - CF_3SO_3$) 1303.1333, found 1303.1331.

(j) [RhOs(CO)$_2$(η^1:η^1-CH_2CH_2C(CO_2Me)=C(CO_2Me))(μ-CO)(dppm)$_2$][CF_3SO_3] (14). Diazomethane, generated from Diazald (50 mg, 0.23 mmol, 16 equiv), was passed through a CH_2Cl_2 solution (10 mL) of **3** (20 mg, 0.014 mmol) at ambient temperature, resulting in an immediate color change from orange to yellow. After stirring for 30 min, the yellow solid was precipitated by the addition of 10 mL of diethyl ether and 50 mL of pentane, filtered, and dried in vacuo (yield 78%). HRMS: *m/z* calc for $C_{61}H_{54}O_7P_4RhOs$($M^+ - CF_3SO_3$) 1317.1490, found 1317.1487.

(k) [RhOs(CO)(η^1:η^1-CH_2CH_2C(CO_2Me)=C(CO_2Me))(μ-CO)$_2$(dppm)$_2$][CF_3SO_3] (15). Method (i). A sample of **14** in CD_2Cl_2 in an NMR tube was left for 2 weeks, after which quantitative conversion to **15** was observed by NMR spectroscopy. **Method (ii).** A THF solution (30 mL) of **14** (20 mg, 0.014 mmol) was heated at reflux for 1 h, after which quantitative conversion to **15** was observed by NMR spectroscopy. Addition of 10 mL of ether and 30 mL of pentane yielded a yellow solid, which was filtered and dried in vacuo to give the compound in 89% yield. HRMS: *m/z* calcd for $C_{61}H_{54}O_7P_4RhOs$ ($M^+ - CF_3SO_3$) 1317.1490, found 1317.1489.

(l) Reaction of 4 + CH_2N_2. An excess of diazomethane generated from Diazald (50 mg, 0.23 mmol, 17 equiv) was passed through a CH_2Cl_2 solution (10 mL) of **4** (20 mg, 0.014 mmol). A rapid color change was observed from yellow to orange. NMR spectroscopy of the resultant solution showed a 1:1 mixture of compounds **6** and **1** based on NMR integration, with a variety of unidentified products.

(m) Attempted Reaction of 12 with HFB. A CD_2Cl_2 solution (0.7 mL) of **12** (20 mg, 0.014 mmol) was prepared at −78 °C, to which an excess of HFB (approximately 0.1 mL) was added. Monitoring of the reaction by ^{31}P NMR indicated no reaction even upon warming to −40 °C. Above this temperature conversion of **12** to **13** occurred with no other reaction observed even upon standing at ambient temperature for days.

(n) Attempted Reaction of 13 with HFB. The sample described in (m) was vented and allowed to warm to ambient temperature. However, after 30 min ^{31}P NMR spectroscopy indicated no reaction had occurred.

(o) Isotopically Labeled Samples. $^{13}CH_2$-enriched samples of the products **5**−**11** were prepared starting with $^{13}CH_2$-labeled **2**, and the labeled compounds **12**−**15** were obtained by reacting **3** with $^{13}CH_2N_2$ generated from ^{13}C-labeled Diazald. ^{13}CO-enriched samples were synthesized from [RhOs(^{13}CO)$_4$(dppm)$_2$][CF_3SO_3].

(p) BF_4^- Salts of Compounds 5 and 15. The BF_4^- salts of both compound **5** and **15** were synthesized exactly as outlined for the triflate analogues in parts (a) and (k), respectively, starting with compounds **2**[11] and **3**[16] as the BF_4^- salts. These samples were used for X-ray structure determinations as outlined in the following section.

(q) PF_6^- Salt of Compound 5. The PF_6^- salt of compound **5** was synthesized as outlined for the triflate analogue in part (a) starting with compound **2** as the PF_6^- salts. Compound **2**-PF_6 was in turn prepared from [RhOs(CO)$_4$(dppm)$_2$][PF_6],[11] which had been prepared as previously reported[16] using aqueous HPF_6 in the protonation step instead of $HBF_4{\cdot}OEt_2$.

X-ray Data Collection and Structure Solution. Pale yellow crystals of [RhOs(CO)$_3$(μ-η^1:η^1-C(CO_2Me)=C(CO_2Me)-CH_2)(dppm)$_2$][BF_4] (**5**)·5.5CH_2Cl_2 were isolated from a solution of dichloromethane-d_2 by slow evaporation in a 5 mm NMR tube. Data for all crystals reported were collected at −80 °C on a Bruker PLATFORM/SMART 1000 CCD diffractometer.[17] Unit cell parameters were obtained from a least-squares refinement of the setting angles of 5423 reflections from the data collection. The space group was determined to be $P\bar{1}$ on the basis of the diffraction symmetry, the lack of systematic absences, and the successful refinement of the structure. The data were corrected for absorption through use of Gaussian integration (indexing of the crystal faces).

The structure of compound **5** was solved using Patterson search and structure expansion (DIRDIF-96),[18] and refinement was completed using the program SHELXL-93.[19] Hydrogen atoms were assigned positions based on the geometries of their attached carbon atoms and were given thermal parameters 20% greater than those of the attached carbons.

Pale yellow crystals containing a 1:1 mixture of [RhOs(CO)$_3$(μ-η^1:η^1-C(CF_3)=C(CF_3)CH_2)(dppm)$_2$][CF_3SO_3] (**6**) and [RhOsCl(CO)$_2$(μ-η^1:η^1-C(CF_3)=C(CF_3)CH_2)(dppm)$_2$] (**7**) together with approximately 1.25 equiv of CH_2Cl_2 were inadvertently coc-

(17) Programs for diffractometer operation, data reduction, and absorption correction were those supplied by Bruker.

(18) Beurskens, P. T.; Beurskens, G.; Bosman, W. P.; de Gelder, R.; Garcia Granda, S.; Gould, R. O.; Israel, R.; Smits, J. M. M. The *DIRDIF-96 program system*; Crystallography Laboratory, University of Nijmegen: The Netherlands, 1996.

(19) Sheldrick, G. M. *SHELXL-93*: Program for crystal structure determination; University of Gottingen: Gottingen, Germany, 1993.

rystallized from a solution in dichloromethane-d_2 by slow evaporation. Unit cell parameters were obtained from a least-squares refinement of the setting angles of 4879 reflections from the data collection. The space group was determined to be $P2_1/n$ (an alternate setting of $P2_1/c$ [No. 14]). The data were corrected for absorption through use of the SADABS procedure.

The structures of compounds **6** and **7** were solved using the direct methods program SHELXS-86[20] and subsequent difference Fourier maps. Refinement was completed using the program SHELXL-93, during which the hydrogen atoms were treated as for compound **5**. The single crystal of this sample was found to contain a 1:1 disordered mixture of compounds **6** and **7**. These molecules were found to be exactly superimposed apart from the overlapping half-occupancy CO and Cl ligands (from compounds **6** and **7**, respectively) on Rh. Clearly, the triflate counterion is also only present as half-occupancy. Superimposed upon the half-occupancy triflate anion is a CH_2Cl_2 solvent molecule of approximate occupancy of 0.25. Refinement, including this solvent molecule, proceeded well, resulting in significant improvements to the *R*-factors and the residual density difference map. Although smeared-out residual electron density still remained in the vicinity of the anion, probably due to additional disordered solvent molecules, we were unable to adequately fit this density to additional solvent. The triflate anion and this disordered solvent occupy a large void centered about 0.7, 1/2, 1/2 in the unit cell that is created by the dppm phenyl rings of adjacent molecules. This void is occupied either by anion or CH_2Cl_2 solvent. In addition, a half-occupancy CH_2Cl_2 molecule at approximately the 1, 1/2, 1/2 position in the unit cell is too close to the triflate anion (Cl−O distance = 2.16 Å) so must be present when the triflate is not, indicating that this void is occupied either by the anion or by a number of disordered CH_2Cl_2 molecules of fractional occupancy. In addition, a smaller void centered at 1/2, 0, 1/2 is also occupied by a one-half-occupancy CH_2Cl_2 that is inversion disordered. Although it seems unusual to have a neutral complex cocrystalize with an ionic complex, the combination of anion or solvent molecules occupying the voids in the crystal apparently results in a favorable packing environment. Refinement of the structure proceeded normally with all atoms behaving well. Dissolution of the bulk solid showed the presence of only compound **6** via $^{31}P\{^1H\}$ NMR spectroscopy, indicating that only a small number of crystals contained the mixture of both compounds. Presumably the few X-ray-quality crystals have the disordered mixture of **6** and **7**, while the bulk sample, which does not give suitable single crystals, is composed of compound **6**.

Yellow crystals of $[RhOs(CO)_3(\eta^1:\eta^1\text{-}CH_2CH_2C(CO_2Me)=C(CO_2Me))(dppm)_2][BF_4]$ (**15**)·Et_2O were obtained by slow diffusion of diethyl ether into a CH_2Cl_2 solution of the compound. Unit cell parameters were obtained from a least-squares refinement of the setting angles of 7215 reflections from the data collection. The space group was determined to be $P2_1/n$. Data were corrected for absorption through use of the SADABS procedure.

The structure of compound **15** was solved using direct methods (SHELXS-86).[20] Refinement was completed using the program SHELXL-93.[19] Hydrogen atoms were treated as for compound **5**.

Crystallographic data for compounds **5**, **6**, **7**, and **15** are given in Table 2.

Results and Compound Characterization

(a) C_3- and C_4-Bridged Species from $[RhOs(CO)_3(\mu\text{-}CH_2)(dppm)_2][X]$. The addition of the symmetrical alkynes, dimethyl acetylenedicarboxylate (DMAD) and hexafluorobutyne (HFB), to the methylene-bridged tetracarbonyl complex, $[RhOs(CO)_4(\mu\text{-}CH_2)(dppm)_2][CF_3SO_3]$ (**1**), does not lead to reaction under ambient conditions. However, removal of a carbonyl from this species, through the use of trimethylamine *N*-oxide (TMNO), yields the highly reactive tricarbonyl complex $[RhOs(CO)_3(\mu\text{-}CH_2)(dppm)_2][CF_3SO_3]$ (**2**), which reacts instantly with these alkynes, yielding $[RhOs(CO)_3(\mu\text{-}\eta^1:\eta^1\text{-}C(CO_2Me)=C(CO_2Me)CH_2)(dppm)_2][CF_3SO_3]$ (**5**) and $[RhOs(CO)_3(\mu\text{-}\eta^1:\eta^1\text{-}C(CF_3)=C(CF_3)CH_2)(dppm)_2][CF_3SO_3]$ (**6**), respectively, as shown in Scheme 1. Compound **5** can also be prepared by refluxing a THF solution of **1** with an excess of DMAD.

Each of these new complexes has the expected $^{31}P\{^1H\}$ NMR pattern characteristic of an AA′BB′X spin system (X = ^{103}Rh), with a signal at about δ 25, having a typical $^1J_{RhP}$ coupling of approximately 110 Hz, corresponding to the Rh-bound ends of the diphosphines and a second signal around δ −2 resulting from the Os-bound ends. In the ^{1}H NMR spectrum, two signals between δ 3.9 and 4.7 are observed for the chemically inequivalent dppm methylene protons, indicating that the molecule possesses "front-back" asymmetry on each side of the $RhOsP_4$ plane. The metal-bound CH_2 signal appears at higher field (**5**, δ 1.68; **6**, δ 2.00) showing coupling to only the osmium-bound ends of the diphosphines, as determined by ^{1}H NMR experiments employing selective ^{31}P decoupling, suggesting that alkyne insertion into the Rh−CH_2 bond has occurred. This is supported by the absence of coupling of the methylene group to Rh or to the Rh-bound phosphines. Repeating the reactions using $^{13}CH_2$-enriched compound **2** (**2**-$^{13}CH_2$) yields products that display a high-field triplet at about δ 7 ($^2J_{PC}$ = 7 Hz) in the $^{13}C\{^1H\}$ NMR spectrum, and the absence of Rh coupling further supports the structural formulation shown in Scheme 1. The $^{13}C\{^1H\}$ NMR spectra of ^{13}CO-labeled samples of **5** and **6** show three terminal carbonyl ligands; two resonances at ca. δ 182 and 171 correspond to the pair of Os-bound carbonyls, while the third at δ 191 corresponds to the Rh-bound carbonyl and displays 50 Hz coupling to this metal.

An X-ray structural determination of **5** confirms that insertion of the alkyne into the Rh−CH_2 bond has taken place, and a representation of the complex cation is shown in Figure 1. Selected bond lengths and angles are presented in Table 3. The dppm ligands occupy their typical trans-bridging positions on both metals. The Os center has a relatively undistorted octahedral geometry in which two sites are occupied by the dppm ligands, one carbonyl lies opposite the Rh−Os bond, while the second carbonyl is trans to the methylene group of the C_3-bridged fragment. At rhodium, the geometry is a square-based pyramid in which the four basal sites are occupied by the phosphines and the carbonyl that is trans to one of the carbons of the inserted alkyne. A vacant coordination site on Rh lies opposite the metal−metal bond. This complex cation is significantly twisted about the metal−metal axis into a staggered conformation with the resulting torsion angles ranging from 25.4(3)° to 28.12(8)°. Within the C_3 fragment, the variation in C−C bond lengths is consistent with the formulation shown in Scheme 1; the C(6)−C(5) bond length (1.33(1) Å) is typical of a C=C double bond, while C(4)−C(5) (1.51(1) Å) is typical of a single bond between sp^3 and

(20) Sheldrick, G. M. *Acta Crystallogr. Sect. A* **1990**, *46*, 467.

Table 2. Crystallographic Data for Compounds 5, 6/7,[a] and 15

compd	$[RhOs(CO)_3(\mu\text{-}\eta^1\text{:}\eta^1\text{-}RC{=}C(R)CH_2)(dppm)_2][BF_4]$ (**5**)[b]·5.5CH_2Cl_2	$[RhOsX(CO)_2(\mu\text{-}\eta^1\text{:}\eta^1\text{-}RC{=}C(R)CH_2)(dppm)_2][CF_3SO_3]_{0.5}$[a,c] (**6/7**)·1.25$CH_2Cl_2$	$[RhOs(CO)_3(\eta^1\text{:}\eta^1\text{-}CH_2CH_2C(R){=}CR)(dppm)_2][BF_4]$[b] (**15**)·$Et_2O$
formula	$C_{65.5}H_{63}BCl_{11}F_4O_7OsP_4Rh$	$C_{59.25}H_{48.5}Cl_3F_{7.5}O_4OsP_4RhS_{0.5}$	$C_{65}H_{64}BF_4O_8OsP_4Rh$
fw	1855.91	1506.35	1476.96
cryst dimens (mm)	0.52 × 0.46 × 0.11	0.37 × 0.07 × 0.05	0.33 × 0.10 × 0.07
cryst syst	triclinic	monoclinic	monoclinic
space group	$P\bar{1}$ (#2)	$P2_1/n$ (alternate setting of $P2_1/c$ (#14))	$P2_1/n$ (alternate setting of $P2_1/c$ (#14))
unit cell param			
a (Å)	12.458(1)[d]	12.3863(8)[e]	12.625(1)[f]
b (Å)	15.222(2)	18.981(1)	28.170(2)
c (Å)	20.881(2)	25.967(2)	17.306(1)
α (deg)	90.438(2)		
β (deg)	92.241(2)	97.086(1)	91.078(2)
γ (deg)	107.474(2)	-	-
V (Å^3)	3773.3(7)	6058.2(7)	6153.6(8)
Z	2	4	4
ρ_{calc} (g cm^{-3})	1.633	1.652	1.594
μ (mm^{-1})	2.434	2.691	2.502
diffractometer		Bruker PLATFORM/SMART 1000 CCD	
radiation (λ (Å))		graphite-monochromated Mo Kα (0.71073)	
temp (°C)	−80	−80	−80
scan type	ω scans (0.2°) (30 s exposures)	ω scans (0.2°) (25 s exposures)	ω scans (0.2°) (40 s exposures)
data collection limit	52.92	52.76	52.84
total data collected	19 250 ($-15 \le h \le 15$, $-18 \le k \le 19$, $-26 \le l \le 20$)	34 347 ($-15 \le h \le 13$, $-22 \le k \le 23$, $-32 \le l \le 32$)	46 114 ($-15 \le h \le 15$, $-35 \le k \le 35$, $-21 \le l \le 21$)
no. of indep reflns	15 127 (R_{int} = 0.0420)	12 407 (R_{int} = 0.0560)	12 592 (R_{int} = 0.0685)
no. of obsd refns (NO)	11 686 ($F_o^2 \ge 2\sigma(F_o^2)$)	9376 ($F_o^2 \ge 2\sigma(F_o^2)$)	9450 ($F_o^2 \ge 2\sigma(F_o^2)$)
range in transm factors	0.7756−0.3642	0.8772−0.4359	0.8443−0.4923
no. of data/restraints/parms	15 127 ($F_o^2 \ge -3\sigma(F_o^2)$)/0/865	12 407 ($F_o^2 \ge -3\sigma(F_o^2)$)/28[g]/721	12 592 ($F_o^2 \ge -3\sigma(F_o^2)$)/0/757
largest difference peak and hole (e Å^{-3})	6.580 and −2.831	1.770 and −1.509	1.123 and −0.861
final R indices[h]			
$R_1(F_o^2 \ge 2\sigma(F_o^2))$	0.0735	0.0498	0.0433
wR_2(all data)	0.2007	0.1323	0.0998
goodness of fit (S)[i]	1.132	1.053	1.113

[a] Compounds **6** and **7** are 50:50 disordered. X = CO in one disordered molecule and Cl in the other. [b] R = CO_2Me. [c] R = CF_3. [d] Obtained from least-squares refinement of 5423 reflections with 4.76° < 2θ < 52.81°. [e] Obtained from least-squares refinement of 4879 reflections with 4.29° < 2θ < 52.38°. [f] Obtained from least-squares refinement of 7215 reflections with 4.34° < 2θ < 52.34°. [g] The S−O, S−C, C−F, O···O, F···F, and O···F (excluding trans O···F) distances of the triflate anion were restrained to be 1.45(1), 1.80(1), 1.35(1), 2.37(1), 2.20(1), and 3.04(1) Å, respectively. The C−O and Cl···Cl distances of the dichloromethane molecules were restrained to be 1.80(1) and 2.95(1) Å, respectively. [h] $R_1 = \Sigma||F_o| - |F_c||/\Sigma|F_o|$; $wR_2 = [\Sigma w(F_o^2 - F_c^2)^2/\Sigma w(F_o^4)]^{1/2}$. [i] $S = [\Sigma w(F_o^2 - F_c^2)^2/(n - p)]^{1/2}$ (n = number of data; p = number of parameters varied; $w[\delta^2(F_o^2) + (AP)^2 + BP]^{-1}$ where $P = [\mathrm{Max}(F_o^2,0) + 2F_c^2]/3$. For compound **5**, A = 0.1067, B = 16.5265; for compounds **6/7**, A = 0.0664, B = 14.7689; for compound **15**, A = 0.0443, B = 1.9039.

Scheme 1

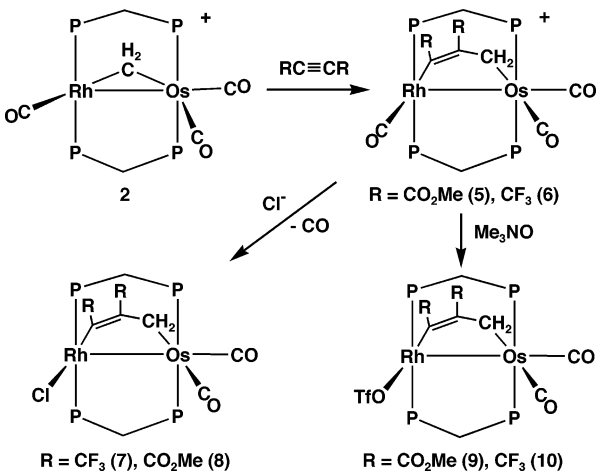

sp^2 carbons.[21] The angles within the C_3 unit also reflect the proposed hybridizations, in which the Rh−C(6)−C(5) and C(6)−C(5)−C(4) angles (124.3(7)°, 122.4(8)°) are typical of sp^2 carbons, while the Os−C(4)−C(5) angle (113.9(5)°) is closer to that expected for sp^3 hybridization. However, all angles are somewhat larger than the idealized values, and together with the acute angles at

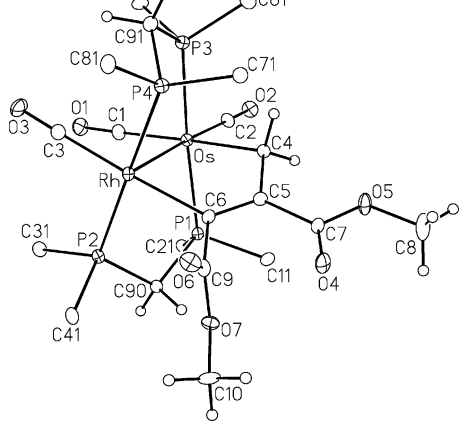

Figure 1. Perspective view of the cation of $[RhOs(CO)_3(\mu\text{-}\eta^1\text{:}\eta^1\text{-}(CO_2Me)C{=}C(CO_2Me)CH_2)(dppm)_2][CF_3SO_3]$ (**5**). Thermal ellipsoids are shown at the 20% probability level except for hydrogens, which are shown artificially small. Only the ipso carbons of the dppm phenyl rings are shown.

(21) Allen, F. H.; Kennard, O.; Watson, D. G.; Brammer, L.; Orpen, A. G.; Taylor, R. *J. Chem. Soc., Perkin Trans. 2* **1987**, S1.

Table 3. Selected Bond Lengths and Angles for Compound 5

(a) Distance (Å)

atom 1	atom 2	distance	atom 1	atom 2	distance
Os	Rh	2.7915(7)	C(1)	O(1)	1.13(1)
Os	C(1)	1.949(9)	C(2)	O(2)	1.11(1)
Os	C(2)	1.864(9)	C(3)	O(3)	1.13(1)
Os	C(4)	2.180(8)	C(4)	C(5)	1.51(1)
Rh	C(3)	1.91(1)	C(5)	C(6)	1.33(1)
Rh	C(6)	2.067(9)			

(b) Angles (deg)

atom 1	atom 2	atom 3	angle	atom 1	atom 2	atom 3	angle
Rh	Os	C(1)	92.0(3)	Os	C(1)	O(1)	178.2(9)
Rh	Os	C(2)	174.6(3)	Os	C(2)	O(2)	179.0(8)
Rh	Os	C(4)	83.1(2)	Rh	C(3)	O(3)	175.7(9)
C(1)	Os	C(2)	93.4(4)	Os	C(4)	C(5)	113.9(5)
C(1)	Os	C(4)	175.1(3)	C(4)	C(5)	C(6)	122.4(8)
C(2)	Os	C(4)	91.5(3)	C(4)	C(5)	C(7)	118.7(7)
Os	Rh	C(3)	93.9(3)	C(6)	C(5)	C(7)	118.7(8)
Os	Rh	C(6)	83.6(2)	Rh	C(6)	C(5)	124.3(7)
C(7)	O(5)	C(8)	115.4(8)	Rh	C(6)	C(9)	113.3(6)
C(9)	O(7)	C(10)	116.1(7)	C(5)	C(6)	C(9)	122.0(8)

the metals (Rh−Os−C(4) = 83.1(2)°; Os−Rh−C(6) = 83.6(2)°) suggest significant strain within the dimetallacyclopentene moiety. This strain is probably responsible for the staggered arrangement of the ligands at both metals, as noted above. An eclipsed conformation, while maintaining the Rh−Os separation, would require the angles within the metallacycle to open up even further from the idealized values, creating even greater strain within this dimetallacycle. The difference in the Os−C(4) (2.180(8) Å) and Rh−C(6) (2.067(9) Å) distances probably reflects the differences in hybridization of these carbons, although some additional shortening of the Rh−C(6) bond may result from π-back-donation into an olefinic π^* orbital. The metal−metal distance of 2.7915(7) Å is typical of a single bond and is significantly shorter that the intraligand P−P distances (ca. 3.04 Å), suggesting a substantial attraction of the metals. We view the metal−metal interaction as a dative bond resulting from donation of the pair of electrons in the Rh d_{z^2} orbital into a vacant Os orbital, giving the latter metal its favored 18e configuration. In this bonding formulation, Rh is in the +1 oxidation state, while Os is +2, representing common oxidation states for these metals.

Attempts to obtain X-ray quality crystals of compound **6** met with repeated failure except on one occasion when a few X-ray quality crystals were found among the bulk sample crystallized from CD_2Cl_2. However, determination of the structure has established that the crystal analyzed is comprised of disordered molecules of the targeted compound **6** together with [RhOsCl(CO)$_2$(μ-η^1:η^1-C(CF$_3$)=C(CF$_3$)CH$_2$)(dppm)$_2$] (**7**) present in the crystal in equal amounts. Presumably, the latter product results from chloride abstraction from the solvent. Although we have not carried out a rational synthesis of **7**, the analogous species derived from **5** has been prepared as outlined later. A representation of compound **6** is not shown since its structure is quite similar to that of compound **5** (shown in Figure 1) and apart from the Rh-bound Cl or CO ligands is superimposable with the chloro compound **7**, which is shown in Figure 2. Bond lengths and angles for the disordered compounds **6/7** are presented in Table 4. The structures of compounds **6** and **7** are very similar to that of **5**,

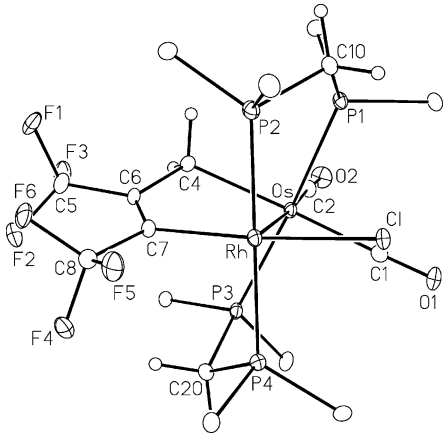

Figure 2. Perspective view of [RhOsCl(CO)$_2$(μ-η^1:η^1-(CF$_3$)C=C(CF$_3$)CH$_2$)(dppm)$_2$] (**7**). Thermal ellipsoids as in Figure 1. Only the ipso carbons of the dppm phenyl rings are shown.

Table 4. Selected Distances and Angles for Compounds 6/7[a]

(a) Distances (Å)

atom 1	atom 2	distance	atom 1	atom 2	distance
Os	Rh	2.7583(6)	Rh	C(7)	2.053(7)
Os	C(1)	1.931(7)	C(1)	O(1)	1.143(8)
Os	C(2)	1.867(7)	C(2)	O(2)	1.146(8)
Os	C(4)	2.202(6)	C(3)	O(3)[a]	1.02(2)
Rh	Cl[a]	2.416(6)	C(4)	C(6)	1.49(1)
Rh	C(3)[a]	1.90(2)	C(6)	C(7)	1.35(1)

(b) Angles (deg)

atom 1	atom 2	atom 3	angle	atom 1	atom 2	atom 3	angle
Rh	Os	C(1)	89.4(2)	Cl	Rh	C(7)[a]	173.2(2)
Rh	Os	C(2)	176.2(2)	C(3)	Rh	C(7)[a]	173.8(6)
Rh	Os	C(4)	83.5(2)	Os	C(4)	C(6)	113.4(4)
C(1)	Os	C(2)	93.6(3)	C(4)	C(6)	C(5)	113.1(6)
C(1)	Os	C(4)	172.9(3)	C(4)	C(6)	C(7)	122.3(6)
C(2)	Os	C(4)	93.5(3)	C(5)	C(6)	C(7)	124.1(6)
Os	Rh	Cl[a]	99.1(1)	Rh	C(7)	C(6)	124.2(5)
Os	Rh	C(3)[a]	94.4(7)	Rh	C(7)	C(8)	112.7(5)
Os	Rh	C(7)	85.3(2)	C(6)	C(7)	C(8)	122.9(6)

[a] Compounds **6** and **7** are 50:50 disordered. C(3)O(3) correspond to compound **6**; Cl corresponds to compound **7**.

confirming that insertion of the HFB molecule into the Rh−CH$_2$ bond has occurred, yielding the C$_3$-bridged "C(CF$_3$)=C(CF$_3$)CH$_2$" moiety. Again the structures of **6** and **7** are staggered along the Rh−Os bond with torsion angles ranging from 22.7(3)° to 28.95(7)°. All parameters for these compounds are in excellent agreement with those of **5**. The C(6)−C(7) distance (1.35(1) Å) of the original alkyne group is consistent with a double bond, while the link between this and the methylene group (C(6)−C(4)), at 1.49(1) Å, is consistent with a single bond. All angles within the dimetallacycle are also in good agreement with those of **5** and again suggest strain that results in skewing of the structure about the metal−metal bond.

The reaction of **5** with Et$_4$NCl yields the chloro complex [RhOsCl(CO)$_2$(μ-η^1:η^1-RC=C(R)CH$_2$)(dppm)$_2$] (R = CO$_2$Me (**8**)), analogous to compound **7**, in which a Rh-bound carbonyl has been replaced by the added chloride ion. An X-ray structure determination of this species confirmed the proposed structure, which is closely comparable to compound **7**. Owing to this similarity and to the poorer diffraction quality of crystals of **8**, its structural parameters are not reported

herein, but full details are given in the Supporting Information.

Carbonyl removal from the triflate salts of compounds **5** and **6** by reaction with trimethylamine *N*-oxide results in triflate ion coordination to yield the neutral species $[RhOs(CF_3SO_3)(CO)_2(\mu\text{-}\eta^1\text{:}\eta^1\text{-}C(CO_2Me)=C(CO_2Me)CH_2)(dppm)_2]$ (**9**) and $[RhOs(CF_3SO_3)(CO)_2(\mu\text{-}\eta^1\text{:}\eta^1\text{-}C(CF_3)=C(CF_3)CH_2)(dppm)_2]$ (**10**), respectively, as diagrammed in Scheme 1. We assume that these triflate-coordinated species are structurally analogous to the chloro adducts **7** and **8**, containing the triflate anion instead of chloride. The $^{31}P\{^1H\}$ NMR spectra of both compounds (**9** and **10**) suggest that they are fluxional at room temperature, as the signals for both sets of phosphines are very broad. Cooling the solutions to −80 °C allows the observation of the low-temperature limiting spectra of these species, which appear as patterns typical of an ABCDX spin system (X = ^{103}Rh) in the $^{31}P\{^1H\}$ NMR spectra in which the Rh-bound phosphines appear as overlapping multiplets between δ 26 and 29, while the Os-bound phosphines appear between δ −4 and −5. This fluxionality presumably occurs via rapid twisting of the molecule about the Rh/Os bond, resulting in the observed broad resonances. In the ground-state structure, in which the metal coordination planes are staggered, the phosphines on Rh are inequivalent since one lies closer to an Os-bound carbonyl while the other is closer to the Os-bound CH_2 group. Twisting about the Rh−Os bond exchanges these environments. Clearly, the structures observed for compounds **5** and **6** should also give rise to an ABCDX pattern, although this was not observed, even at −80 °C. We assume that in these cases the smaller carbonyl allows the fluxional process to occur readily over the full temperature range investigated. It is noteworthy that the analogous chloro species (**8**) also displays an ABCDX pattern in the $^{31}P\{^1H\}$ NMR spectrum at −80 °C; again it appears that the larger anion (compared to CO) allows the low-temperature limiting structure to be observed.

The osmium-bound methylene signal in **9** remains a triplet at δ 1.08 in the ^{1}H NMR spectrum, with coupling to only the Os-bound phosphines observed. The two carbonyl ligands appear in the $^{13}C\{^1H\}$ NMR spectrum at δ 181.8 and 171.5 with 2-bond coupling to the Os-bound ^{31}P nuclei of 5 and 11 Hz, respectively. Small coupling (1−3 Hz) to Rh is also observed for both carbonyls, and these are proposed to come about via coupling through the metal−metal bond. The absence of carbonyl ligands on Rh results in electron deficiency at this metal, and therefore it is proposed that the triflate ion is coordinated to Rh, similar to that observed for the chloride ion in **7** and **8**. Replacement of a carbonyl by triflate or chloride anion has resulted in a significant drop in the stretching frequencies of the remaining carbonyls, as shown in Table 1.

Attempts to remove a carbonyl from $[RhOs(CO)_3(\mu\text{-}\eta^1\text{:}\eta^1\text{-}C(R)=C(R)CH_2)(dpppm)_2][PF_6]$ (R = CO_2Me (**5**-PF_6)), in which the triflate anion has been replaced by the noncoordinating PF_6^- anion, yielded **8** as the major species (together with unidentified species) when carried out in CH_2Cl_2. Clearly, the solvent is the source of the coordinated chloro ligand in the product. Attempts to carry out carbonyl removal in nitromethane, thereby avoiding the potential of the chloride ion participation, yielded a mixture of unidentified products.

Scheme 2

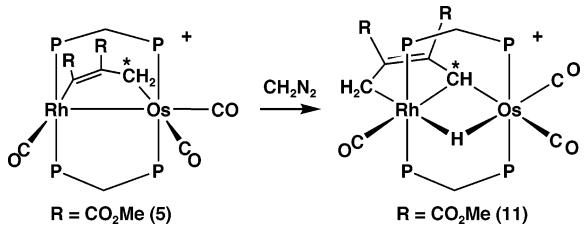

Although compound **6** does not react further with diazomethane, compound **5** does react to yield the C_4-bridged product $[RhOs(CO)_3(\mu\text{-}\eta^1\text{:}\eta^1\text{-}CH_2C(CO_2Me)=C(CO_2Me)CH)(\mu\text{-}H)(dppm)_2][CF_3SO_3]$ (**11**), shown in Scheme 2. The ^{1}H NMR spectrum of **11** displays a resonance corresponding to two hydrogens, at δ 4.07, with coupling of 2 Hz to Rh and 11 Hz to the Rh-bound phosphines, indicating that a methylene group has inserted into the Rh−alkyne bond. A signal at δ 5.29, integrating as one proton and displaying 2 Hz coupling to Rh and 4 Hz coupling to the Os-bound ^{31}P nuclei, corresponds to the single hydrogen of the original methylene group. The other proton originating from the methylene group of **5** now bridges the metals, as is indicated by the signal at δ −16.6, which displays coupling to all four ^{31}P nuclei and Rh. When a $^{13}CH_2$-enriched sample of **5** (generated from $^{13}CH_2$-enriched **2**) is reacted with $^{12}CH_2N_2$, the ^{13}C label occupies only the bridging CH site for which the single hydrogen at δ 5.29 displays 161 Hz coupling to this ^{13}C nucleus. The $^{13}C\{^1H\}$ NMR signal of this μ-CH moiety appears at δ 118.3 and displays 16 Hz coupling to Rh, while the signal for the new unenriched CH_2 group is found at δ 70.3 with 25 Hz coupling to Rh. These data clearly indicate that the added methylene group is bound to Rh, while the original CH_2 group of compound **5** has undergone C−H activation to yield the alkylidene-bridged group and the bridging hydride. The chemical shift for this alkylidene carbon and the C−H coupling constant are consistent with previous determinations.[15,22] Although the top/bottom asymmetry of **11**, by virtue of the unsymmetrical bridging alkylidene group, should give rise to a complex pattern in the $^{31}P\{^1H\}$ NMR spectrum of an ABCDX (X = ^{103}Rh) spin system, this spectrum at ambient temperature is deceptively simple, appearing as an AA′BB′X spin system. Upon cooling to −80 °C the spectrum becomes more complex as new peaks appear, but the chemical shifts for the pair of Rh-bound phosphorus nuclei are superimposed, as are those for the Os-bound ends.

(b) C_3- and C_4-Bridged Species from $[RhOs(CO)_3(\mu\text{-}\eta^1\text{:}\eta^1\text{-}C(R)=C(R))(dppm)_2][X]$. The alkyne-bridged species $[RhOs(CO)_3(\mu\text{-}\eta^1\text{:}\eta^1\text{-}C(R)=C(R))(dppm)_2][CF_3SO_3]$ (R = CO_2Me (**3**), CF_3 (**4**)) have been previously reported,[16] and we now find that both species react with diazomethane, although they yield very different products. In the reaction of compound **3** with CH_2N_2 three different products are obtained depending upon the reaction conditions. At −80 °C, the reaction with diazomethane yields $[RhOs(CO)_3(\mu\text{-}\eta^1\text{:}\eta^1\text{-}CH_2C(CO_2Me)=$

(22) Torkelson, J. R.; McDonald, R.; Cowie, M. *Organometallics* **1999**, *18*, 4134.

Scheme 3

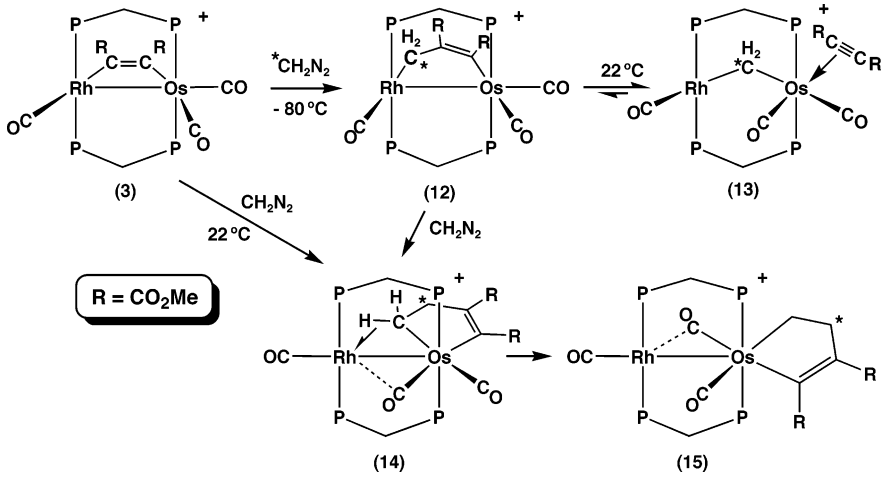

C(CO_2Me))(dppm)$_2$][CF_3SO_3] (**12**), in which methylene insertion into the Rh−alkyne bond has occurred, as diagrammed in Scheme 3. Compound **12** is an isomer of **5** in which the attachment of the hydrocarbyl unit to Rh and Os is reversed. Isolation of this species at ambient temperature was not possible owing to its facile conversion to a new product (**13**) (vide infra), so it was characterized by NMR spectroscopy at −80 °C. The added methylene group appears as a triplet at δ 4.82 ($^3J_{P(Rh)H}$ = 7 Hz) in the ^{1}H NMR spectrum, while in the ^{13}C{^{1}H} NMR spectrum it appears at δ 103.6 and displays 28 Hz coupling to Rh, confirming that it has inserted into the Rh−alkyne bond. Three terminally bound carbonyls are present at δ 200.4 ($^1J_{RhC}$ = 49 Hz, $^2J_{PC}$ = 14 Hz), 192.9, and 176.6 ($^2J_{PC}$ = 9 Hz), consistent with the structure shown in Scheme 3, in which one is bound to Rh and two are Os bound. As will be seen throughout this paper, and as has been described elsewhere,[23] the high-field, Os-bound carbonyl corresponds to the one that lies remote from Rh, while the low-field carbonyl on this metal is the one that is adjacent to Rh. The dppm resonances, in both the ^{1}H and ^{31}P{^{1}H} NMR spectra, are typical for such compounds.

Warming a sample of **12** to ambient temperature in the absence of excess diazomethane results in the formation of **13**, which appears to have resulted from deinsertion of the alkyne, leaving the methylene group bridging the metals and the alkyne adjacent to it bound to Os in an η^2 manner. The two inequivalent methyl signals of the DMAD ligand appear in the ^{1}H NMR spectrum as singlets at δ 3.72 and 2.10. Three methylene signals appear in the ^{1}H NMR spectrum of compound **13**; two signals at δ 4.01 and 3.89 correspond to the dppm groups, while the metal-bound CH_2 group appears at δ 1.32 ($^1J_{CH}$ = 128 Hz) and shows coupling to both sets of phosphines, confirming that it is in a bridging position. This bridging methylene carbon was observed at δ 30.6 in the ^{13}C{^{1}H} NMR spectrum and was found to have 18 Hz coupling to Rh and 8 Hz coupling to the Rh-bound ^{31}P nuclei (although the absence of coupling between the $^{13}CH_2$ group and the Os-bound ^{31}P nuclei may appear inconsistent with our formulation, we frequently do not observe ^{13}C−^{31}P coupling involving Os-bound groups). The Rh-bound carbonyl appears as a doublet of triplets at δ 190.8 ($^1J_{RhC}$ = 52 Hz, $^2J_{PC}$ = 12 Hz), while two multiplets at δ 190.7 and 169.6 result from the Os-bound carbonyls. The high-field, osmium-bound carbonyl is again assigned to the one not in the immediate vicinity of Rh, whereas the low-field signal (δ 190.7) indicates that this group lies in the vicinity of the adjacent Rh center, although not necessarily formally bound to it.[23] This arrangement defines that there will be no other ligand between this carbonyl and Rh, ruling out the presence of another bridging group. The structure shown for **13**, having the alkyne adjacent to the bridging methylene group, is consistent with the reversibility of the alkyne deinsertion step (**12** ⇌ **13**) that is proposed on the basis of the subsequent reaction of **13** with diazomethane (vide infra). It is not clear why isomer **5**, having the unsaturated end of the C_3 fragment bound to Rh and the saturated end bound to Os, is stable, whereas isomer **12**, having the opposite arrangement, is unstable to alkyne deinsertion.

Addition of diazomethane to either **3** or **13** at ambient temperature or allowing **12** to warm to ambient temperature in the presence of CH_2N_2 yields [$RhOs(CO)_2$-(μ-η^1:η^1-$CH_2CH_2C(CO_2Me)$=$C(CO_2Me)$)(μ-CO)(dppm)$_2$]-[CF_3SO_3] (**14**), in which an osmacyclopentene moiety has formed having an agostic interaction involving one of the methylene groups and Rh as diagrammed in Scheme 3. In the ^{1}H NMR spectrum the two sets of diazomethane-generated methylene groups are observed as two broad multiplets at δ 3.52 and 0.89. ^{1}H{^{31}P} NMR experiments show that the multiplet at δ 0.89 has coupling to Rh of 4 Hz in addition to unresolved couplings to all ^{31}P nuclei, and therefore this is assigned to the methylene group having the agostic interaction with Rh; the multiplet at δ 3.52 shows coupling to neither the dppm ligands nor Rh and is therefore assigned to the methylene group that is bonded to the alkyne moiety. The agostic interaction of the methylene group with Rh is proposed on the basis of the reduced $^1J_{CH}$ coupling constant of 116 Hz observed when ^{13}-CH_2N_2 is used to prepare **14**. By comparison, the C−H coupling constant for the other methylene group is 128 Hz. The observation of only one hydrogen resonance for this terminal CH_2 group leads us to propose that both hydrogens of the agostic methylene group are alternat-

(23) George, D. S. A.; McDonald, R.; Cowie, M. *Organometallics* **1998**, *17*, 2553.

ing between an agostic and a terminal position, yielding a reduced C−H coupling constant that is simply an average of the coupling observed in these two positions. If a value of $^1J_{CH} = 130$ Hz for the terminal bond is assumed, the coupling constant of the agostic interaction can be calculated to be 102 Hz, which is consistent with previous reports.[24]

The $^{13}C\{^1H\}$ NMR spectrum of a fully $^{13}CH_2$-labeled sample of **14** shows a signal at δ −7.59 that exhibits 4 Hz coupling to Rh and is assigned to the metal-bound methylene that is involved in the agostic interaction, while a resonance at δ 41.80 with no Rh or P coupling is assigned to the other methylene group. Both carbons exhibit mutual coupling of 32 Hz. Three carbonyl resonances are observed in the $^{13}C\{^1H\}$ NMR spectrum when ^{13}CO-labeled **14** is prepared: a resonance at δ 176.7 is assigned as terminally bound to Os, one at δ 186.7 is assigned as terminally bound to Rh, as demonstrated by its large coupling to rhodium ($^1J_{RhC} = 84$ Hz), while the third at δ 193.4 is assigned as semibridging, showing a small coupling to Rh of 9 Hz. This arrangement is supported by IR spectroscopy, which shows two stretches due to terminal carbonyls and one for a bridging carbonyl at 1870 cm^{-1}. The structure proposed for compound **14** is analogous to that of $[RhOs(CO)_3(\eta^1{:}\eta^1\text{-}C_4H_8)(dppm)_2]^+$, which resulted from the coupling of four methylene groups, the structure of which was established crystallographically.[11] Not surprisingly, the spectral characteristics of both species are closely comparable.

Over a period of several weeks at ambient temperature or 1 h in refluxing THF, **14** transforms into $[RhOs(CO)_2(\eta^1{:}\eta^1\text{-}CH_2CH_2C(CO_2Me){=}C(CO_2Me))(\mu\text{-}CO)(dppm)_2][CF_3SO_3]$ (**15**), as shown in Scheme 3. Compound **15** has maintained the osmacyclopentene structure of its precursor, although the agostic interaction with Rh is no longer present. The two pairs of methylene protons of the osmacyclopentene are seen to overlap at δ 1.87 in the ^1H NMR spectrum; however two resolved signals appear for these groups in the $^{13}C\{^1H\}$ NMR spectrum. The Os-bound CH_2 is observed as a triplet ($^2J_{PC} = 6$ Hz) at δ 10.2, while the other is a singlet at δ 39.7. Also in the $^{13}C\{^1H\}$ NMR spectrum the Rh-bound carbonyl appears at δ 182.1 ($^1J_{RhC} = 82$ Hz), while two other signals at δ 190.5 and 201.7 result from the pair of inequivalent osmium-bound carbonyls. We assume that the higher-field signal corresponds to a carbonyl having no formal bonding interaction with Rh,[23] in keeping with the absence of Rh coupling observed for this group, while the low-field signal shows a weak coupling of 9 Hz and is designated as semibridging.

The structure of **15**, as the BF_4^- salt, has been determined by X-ray crystallographic methods, and a representation of the complex cation is shown in Figure 3, with selected bond lengths and angles given in Table 5. An osmacyclopentene fragment, consisting of two coupled methylene units, a molecule of DMAD, and the Os center, lies in the plane perpendicular to the dppm ligands. The Rh−Os bond distance of 2.8464(5) Å is typical of a metal−metal single bond and is shorter than the nonbonded P···P distances (ca. 3.04 Å), suggesting

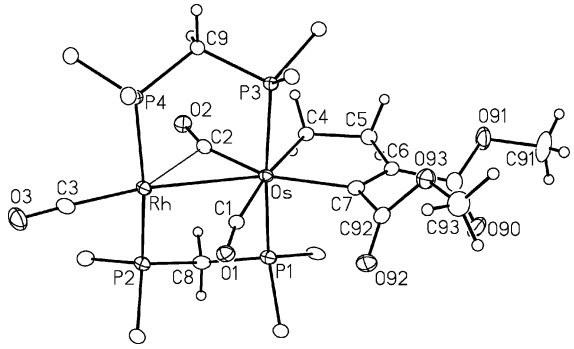

Figure 3. Perspective view of the cation of $[RhOs(CO)_3(\mu\text{-}\eta^1{:}\eta^1\text{-}CH_2CH_2C(CO_2Me){=}C(CO_2Me))(dppm)_2][CF_3SO_3]$ (**15**). Thermal ellipsoids as in Figure 1. Only the ipso carbons of the dppm phenyl rings are shown.

Table 5. Selected Distances and Angles for Compound 15

(a) Distances (Å)

atom 1	atom 2	distance	atom 1	atom 2	distance
Os	Rh	2.8464(5)	Rh	C(3)	1.868(6)
Os	C(1)	1.960(5)	C(1)	O(1)	1.153(6)
Os	C(2)	1.946(6)	C(2)	O(2)	1.165(6)
Os	C(4)	2.192(5)	C(3)	O(3)	1.133(6)
Os	C(7)	2.129(5)	C(4)	C(5)	1.533(7)
Rh	C(1)	2.487(5)	C(5)	C(6)	1.481(7)
Rh	C(2)	2.252(5)	C(6)	C(7)	1.340(7)

(b) Angles (deg)

atom 1	atom 2	atom 3	angle	atom 1	atom 2	atom 3	angle
Rh	Os	C(1)	58.9(2)	Os	Rh	C(3)	165.6(2)
Rh	Os	C(2)	52.0(2)	Os	C(1)	O(1)	171.3(4)
Rh	Os	C(4)	128.2(1)	Os	C(2)	O(2)	158.7(4)
Rh	Os	C(7)	154.3(1)	Rh	C(2)	O(2)	116.3(4)
C(1)	Os	C(2)	110.9(2)	Rh	C(3)	O(3)	176.1(6)
C(1)	Os	C(4)	172.6(2)	Os	C(4)	C(5)	113.8(3)
C(1)	Os	C(7)	95.4(2)	C(4)	C(5)	C(6)	110.5(4)
C(2)	Os	C(4)	76.2(2)	C(5)	C(6)	C(7)	120.2(5)
C(2)	Os	C(7)	153.7(2)	Os	C(7)	C(6)	117.8(4)
C(4)	Os	C(7)	77.5(2)				

mutual attraction of the metals. The Os center has an octahedral arrangement of ligands, while at Rh the geometry is best described as square planar (if the semibridging carbonyl (C(2)O(2)) is ignored). The osmacyclopentene fragment has typical single-bond lengths for Os−C(4) (2.192(5) Å), Os−C(7) (2.129(5) Å), C(4)−C(5) (1.533(7) Å), and C(5)−C(6) (1.481(7) Å), while the C(6)−C(7) bond length (1.340(7) Å) is typical of a double bond. Consistent with the differences noted above in the $^{13}C\{^1H\}$ NMR spectrum for the two Os-bound carbonyls, one (C(1)O(1)) appears to be primarily terminally bound, as shown by its large separation from Rh (Rh−C(1) = 2.487(5) Å) and its close-to-linear arrangement at Os (Os−C(1)−O(1) = 171.3(4)°), while the other (C(2)O(2)) appears to be semibridging, having a shorter Rh−C(2) separation (2.252(5) Å) than Rh−C(1) and a more bent geometry (Os−C(2)−O(2) = 158.7(4)°; Rh−C(2)−O(2) = 116.3(4)°). The slight bend of C(1)O(1) away from Rh suggests a very weak interaction with this adjacent metal.

In an effort to further understand the mechanism of this reaction, an NMR labeling study was carried out whereby $^{13}CH_2N_2$ was reacted with **3** at −78 °C. At this temperature **12**-$^{13}CH_2$ was observed with the labeled methylene group inserted into the Rh−alkyne bond. Upon removal of excess $^{13}CH_2N_2$ in vacuo and warming to ambient temperature, **13**-$^{13}CH_2$ was observed with

(24) (a) Jeffery, J. C.; Orpen, A. G.; Stone, F. G. A.; Went, M. J. *J. Chem. Soc., Dalton Trans.* **1986**, 173. (b) Park, J. W.; Mackenzie, P. B.; Schaefer, W. P.; Grubbs, R. H. *J. Am. Chem. Soc.* **1986**, *108*, 6402.

the $^{13}CH_2$ label retained but now in the position bridging the metals. This indicates that the alkyne has deinserted from the C_3-bridged unit of **12** and now occupies an η^2-position on Os. Subsequent addition of unlabeled CH_2N_2 to **13** was found to yield **14** with the labeled carbon adjacent to the alkyne and the added unlabeled CH_2N_2 inserted into the Rh−$^{13}CH_2$ bond. Isomerization of **14** to **15** resulted in the label remaining in the position adjacent to the alkyne. Retention of the $^{13}CH_2$ label adjacent to the alkyne moiety in both **14** and **15** upon reaction of **13** with diazomethane supports the equilibrium noted earlier (**12** ⇌ **13**) whereby **12** is the reactive species that incorporates an additional methylene group.

When the hexafluorobutyne-bridged compound **4** is reacted with diazomethane, $[RhOs(CO)_4(\mu\text{-}CH_2)(dppm)_2][CF_3SO_3]$ (**1**) and $[RhOs(CO)_3(\mu\text{-}\eta^1\text{:}\eta^1\text{-}C(CF_3)=C(CF_3)CH_2)(dppm)_2][CF_3SO_3]$ (**6**) are observed in an approximate 1:1 ratio as the major products along with minor amounts of unidentified products in the $^{31}P\{^1H\}$ NMR spectrum. Initially, formation of **6** seems somewhat surprising, as it appears that the methylene group has inserted into the Os−alkyne bond, whereas in all previous studies substrate insertion has occurred at Rh.[10c,11,14,15] However, monitoring the reaction by ^{19}F NMR spectroscopy at −80 °C showed the presence of free HFB in solution at intermediate times, indicating that alkyne dissociation is occurring. Presumably, the reaction initially proceeds as noted above for the DMAD analogue with formation of the C_3-bridged intermediate analogous to **12**. Since this species is not observed, extrusion and loss of HFB apparently is extremely facile, for reasons that are not understood. The dissociated alkyne then inserts into the Rh−CH_2 bond as shown in Scheme 1. The formation of the tetracarbonyl complex **1** presumably results from scavenging of a carbonyl from decomposition products.

Discussion

The heterobinuclear complex $[RhOs(CO)_4(dppm)_2][CF_3SO_3]$ has previously been found to add up to four methylene groups to yield either $[RhOs(CO)_4(\mu\text{-}CH_2)(dppm)_2][CF_3SO_3]$, $[RhOs(CO)_3(\eta^1\text{:}\eta^1\text{-}C_4H_8)(dppm)_2][CF_3SO_3]$, or $[RhOs(CH_3)(\eta^1\text{-}C_3H_5)(CO)_3(dppm)_2][CF_3SO_3]$, depending upon conditions.[11] The unusual sequence of methylene-insertion steps leading to these products was proposed to occur by stepwise methylene insertion into the Rh−CH_2 bonds of bridging C_1 to C_3 hydrocarbyl fragments. However, in this chain-building sequence the important putative C_2- and C_3-bridged intermediates were not observed. In attempts to learn more about the possible roles of bridging hydrocarbyl groups in carbon−carbon chain growth in processes such as the Fischer−Tropsch reaction, we chose to use alkynes as model C_2 fragments and to investigate the different C−C bond-forming pathways involving these groups and methylene fragments.

(a) C_3-Bridged Species. Two approaches to methylene and alkyne-group coupling to give C_3-bridged species were obvious: either alkyne insertion into a metal−methylene bond of a bridging CH_2 group in species such as $[RhOs(CO)_n(\mu\text{-}CH_2)(dppm)_2][CF_3SO_3]$ (n = 4 (**1**), 3 (**2**)) or methylene insertion into a metal−carbon bond involving a bridging alkyne group in species such as $[RhOs(CO)_3(\mu\text{-}RC_2R)(dppm)_2][CF_3SO_3]$. In the first approach, the methylene-bridged tetracarbonyl species (**1**) was found to be unreactive with alkynes at ambient temperature. However, carbonyl removal from **1**, either under reflux or in the presence of Me_3NO to give $[RhOs(CO)_3(\mu\text{-}CH_2)(dppm)_2][CF_3SO_3]$ (**2**), resulted in instantaneous reaction of this species with DMAD or HFB, yielding the alkyne-insertion products, $[RhOs(CO)_3(\mu\text{-}\eta^1\text{:}\eta^1\text{-}C(R)=C(R)CH_2)(dppm)_2][CF_3SO_3]$ (R = CO_2Me (**5**), CF_3 (**6**)), as was diagrammed in Scheme 1. These products have resulted from alkyne insertion into the Rh−CH_2 bond of the precursor, and the targeted C_3-bridged species function as effective models for the putative C_3H_6-bridged intermediate in the methylene-coupling sequence reported earlier.[11] This $\eta^1\text{:}\eta^1$-C_3-bridged geometry also models analogous C_3H_6-bridged products of ethylene and methylene coupling proposed by Dry,[7f] Pettit,[8d,f] and others.[8] In most cases the proposed C_3H_6-bridged fragments have not been observed, presumably undergoing facile β-hydrogen elimination, frequently followed by reductive elimination of propene. One advantage of our unsaturated, model C_3-bridged systems is the absence of hydrogens in the central sites that are β to both metals, removing this decomposition pathway, and allowing their isolation, characterization, and further study.

Although the observed bridging "RC=C(R)CH_2" unit (**A**) was our target, in some ways its formation is unusual. Analogous insertions involving alkynes and bridging methylene groups had not previously yielded this fragment but had instead resulted in formation of the vinyl carbene moiety **B**.[9] However, as shown in these

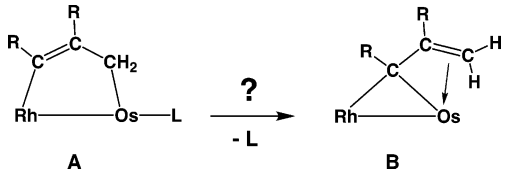

valence-bond formulations, these fragments are closely related, differing only in their binding mode; in **A** the ligand functions as a two-electron donor, while in **B** this group donates four electrons. We therefore speculated that removal of a two-electron donor (L) from **A** might result in a transformation of the hydrocarbyl bridge to yield a species resembling **B**. Carbonyl removal from **5** or **6** did not yield the targeted ligand transformation, resulting instead in anion coordination to give $[RhOs(OSO_2CF_3)(CO)_2(\mu\text{-}\eta^1\text{:}\eta^1\text{-}C(R)=C(R)CH_2)(dppm)_2]$, having structures analogous to those of **5** and **6**. In this way, the triflate anion compensates for loss of the carbonyl, negating the need for rearrangement of the hydrocarbyl fragment. Although we were unable to obtain suitable crystals to allow crystallographic confirmation of these neutral products, the spectroscopy strongly supports this assignment, and the structure determinations of the chloro analogues $[RhOsCl(CO)_2(\mu\text{-}\eta^1\text{:}\eta^1\text{-}C(R)=C(R)CH_2)(dppm)_2]$ (R = CF_3 (**7**), CO_3Me (**8**)) offer additional support, having structures in which the chloro ligand replaces triflate.

The simple transformations of **5** and **6** upon carbonyl removal, involving replacement by triflate anion, is in contrast to that reported earlier by us[15] upon carbonyl removal from the Rh/Ru analogue $[RhRu(CO)_3(\mu\text{-}\eta^1\text{:}\eta^1\text{-}$

$C(CO_2Me)=C(CO_2Me)CH_2)(dppm)_2][CF_3SO_3]$, which yielded $[RhRu(CO)_2(\mu\text{-}\eta^1{:}\eta^3\text{-}CHC(CO_2Me)C(H)CO_2Me)(dppm)_2][CF_3SO_3]$, proposed to occur by a sequence of steps initiated by C−H activation of the Os-bound CH_2 group by the adjacent Rh center.[14] In this proposal, the pivotal first step in the hydrocarbyl group isomerization occurs at Rh, so it is not obvious why the analogous Rh/Os complex behaves differently than the Rh/Ru system. Even substituting the coordinating triflate anion by PF_6^-, which should not coordinate, did not yield the targeted transformation as diagrammed above in the **A** → **B** conversion or the more complex transformation observed for the Rh/Ru analogue.[15] Instead, either chloride ion abstraction from CH_2Cl_2 or decomposition in nonchlorinated solvent occurred. The reasons for the difference in these closely related systems are not clear.

Taking the second approach to C_3-bridged complexes, namely, methylene insertion into the Rh−C bond of an alkyne-bridged species, $[RhOs(CO)_3(\mu\text{-}\eta^1{:}\eta^1\text{-}RC{=}CR)(dppm)_2][CF_3SO_3]$ (**3**), yields $[RhOs(CO)_3(\mu\text{-}\eta^1{:}\eta^1\text{-}CH_2C(R){=}CR)(dppm)_2][CF_3SO_3]$ (R = CO_2Me (**12**)), which is an isomer of **5**, having the hydrocarbyl group reversed such that now the methylene group is adjacent to Rh with one end of the original alkyne still bound to Os (see Scheme 3). Unlike its isomer (**5**), this product is unstable to alkyne deinsertion, yielding the product $[RhOs(CO)_3(\eta^2\text{-}RC{\equiv}CR)(\mu\text{-}CH_2)(dppm)_2][CF_3SO_3]$ (**13**) at ambient temperature. Although **13** is the only species observed at ambient temperature, we propose that it exists in equilibrium with trace amounts of **12** on the basis of the subsequent chemistry of **13**, which is consistent with it reacting via a C_3-bridged species such as **12** (vide infra). Support for this deinserted formulation (beyond the spectroscopy and labeling study discussed earlier) is the analogous reaction of $[RhOs(CO)_3(\mu\text{-}\eta^1{:}\eta^1\text{-}RC{=}CR)(dppm)_2][CF_3SO_3]$ (R = CF_3 (**4**)) with diazomethane in which **6** was observed. We demonstrated that reaction of this HFB-bridged complex (**4**) with diazomethane proceeds via HFB dissociation, presumably from an intermediate analogous to **13**, which readily loses HFB to yield **2**, followed by alkyne insertion into the Rh−CH_2 bond of this species. It appears that loss of dimethyl acetylenedicarboxylate from **13** does not occur. This is supported by the absence of compound **5** in the reaction mixture (which would have resulted from reaction of the alkyne with the methylene-bridged species (**2**) generated). Furthermore, warming samples of either **12** or **13** in the presence of hexafluorobutyne results in no incorporation of this alkyne; only starting materials are observed. It appears that the major differences in the two alkynes are the more facile extrusion of the latter alkyne from the putative C_3-bridged intermediate and the subtly different binding strengths of the alkynes in the extruded products, with DMAD binding more strongly to Os than HFB.

(b) C_4-Bridged Species. Having generated two classes of C_3-bridged species from either the methylene- or alkyne-bridged precursors, both of which serve as unsaturated analogues of the putative C_3H_6-bridged intermediate in our previous methylene-coupling sequence (although one of these (**12**) is admittedly stable only at lower temperature), it was of obvious of interest

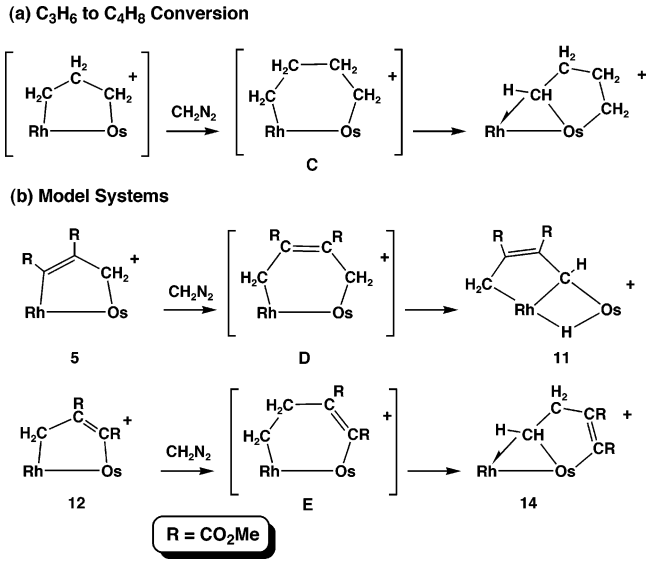

Figure 4. Comparison of the C_3H_6 to C_4H_8 conversion[11] with two model systems. Only the metals and hydrocarbyl fragments are shown.

to build up the hydrocarbyl chain through subsequent methylene insertions. Surprisingly, the HFB-inserted product (**6**) did not react further. However, the DMAD analogue (**5**) reacted readily with diazomethane to give a targeted C_4 product. Although this was not the anticipated product of methylene insertion into the Rh−C bond of **5**, carbon−carbon bond formation did occur, only to be accompanied by C−H bond activation of the Os-bound methylene group. It is not clear why this difference from the C_4H_8 product has occurred, but we assume that it relates to the differing degrees of strain within the two proposed intermediates in these processes, diagrammed as **C** and **D** in Figure 4. We assume that these C_4-bridged products are disfavored by the ring strain. In the case of the C_4H_8-bridged species (**C**) migration to a chelated, terminal site on Os gives a favorable five-membered metallacycle, which is further stabilized by the agostic interaction with Rh. In the case of the unsaturated analogue (**D**) C−H activation of the Os-bound CH_2 group by Rh occurs. C−H activation by a distal metal may seem surprising; however we note that in such a system this CH_2 group is in a β-position with regard to Rh. Furthermore, the twisting observed in compounds **5**, **6**, **7**, and **8** (see Figures 1 and 2 and Figures S1 and S2 in the Supporting Information) brings one proton of the Os-bound CH_2 group into the vicinity of Rh, facilitating activation by this metal. Presumably the additional strain resulting from insertion of the second CH_2 group combined with the unsaturated part of the metallacycle, which prevents puckering that is necessary to alleviate some of the strain, brings this methylene group even closer to Rh, resulting in its activation.

In the case of the "reverse isomer" $[RhOs(CO)_3(\mu\text{-}\eta^1{:}\eta^1\text{-}CH_2C(R){=}CR)(dppm)_2][CF_3SO_3]$ (R = CO_2Me (**12**)), reaction with excess diazomethane upon warming to ambient temperature yields the targeted C_4 product $[RhOs(CO)_3(\eta^1{:}\eta^1\text{-}CH_2CH_2C(R){=}CR)(dppm)_2][CF_3SO_3]$ (**14**), which has an exactly analogous structure to the C_4H_8-containing product noted earlier,[11] even including the agostic interaction of the Os-bound CH_2 group with Rh. This product is also obtained upon reacting com-

pound **13** with diazomethane, in which labeling studies confirm that the original C_3 unit is contiguous in the C_4 product **14** (see Scheme 3). Compound **14** is also obtained in the reaction of **3** under the same conditions and presumably originates from the C_4-bridged intermediate **E** by migration from the bridged to a chelating position on Os. As in the case of the C_4H_8 species, we assume that this transformation is favored by the less strained five-membered ring that results.

A comparison of the three C_3 to C_4 transformations observed in this system, and diagrammed in Figure 4, presents some interesting contrasts based on the nature of the proposed C_4-bridged fragment. In both cases involving the unsaturated substrate the C_3- to C_4-bridged transformation models the C_3H_6- to C_4H_8-bridged transformation very well, with methylene insertion occurring into the Rh−C bond in each case. However, CH_2 insertion into the "Rh(μ-η^1:η^1-RC=C(R)-CH_2)Os" moiety to give **D** behaves somewhat differently, undergoing C−H activation at the Os-bound CH_2 group. As noted earlier, the difference in reactivity of **D** compared to **C** probably originates in the differing strain experienced by the saturated fragment in the latter and the unsaturation in the former. To eliminate this C−H activation pathway, we generated the "Rh(μ-η^1:η^1-CH_2-CH_2(R)C=CR)Os" moiety (**E**), and as anticipated, the absence of an Os-bound CH_2 group allows the "CH_2-CH_2C(R)=CR" moiety to remain intact, giving the unsaturated analogue of [RhOs(CO)$_3$(η^1:η^1-C_4H_8)-(dppm)$_2$][CF_3SO_3].[11] The unsaturated systems model the saturated one in another way. We had proposed that the methylene-coupling sequence had occurred by methylene insertion into a labile Rh−CH_2 bond of a bridging hydrocarbyl group[11] and that termination at a C_4 chain length had resulted from migration of the C_4H_8 group from the bridging site to a chelated arrangement on Os, to relieve the ring strain in the former. In this chelating position on Os the hydrocarbyl group no longer has an adjacent site of unsaturation for activation of additional diazomethane and the stronger Os−CH_2 bond is presumably less susceptible to insertion. In the unsaturated systems described in this study, termination at C_4 species again occurred, and it is proposed that ring strain in the analogous six-membered dimetallacycles is again responsible. In the **E** → **14** transformation migration to a chelating position on Os again occurred, whereas in the **D** → **11** transformation the resulting C−H activation of the strained intermediate led to coordinative saturation at both metals, making subsequent CH_2 insertions impossible.

Conclusions

We have succeeded in modeling the transformations from C_1- to C_4-bridged and from C_2- to C_4-bridged products by the coupling of diazomethane-generated methylene groups and dimethyl acetylenedicarboxylate. As we have previously noted,[11b,14] carbon−carbon bond formation in all cases occurs by substrate insertion into the Rh−carbon bond of the appropriate *hydrocarbyl-bridged* precursor. The subtly different reactivities of the different C_4-bridged intermediates have been rationalized on the basis of different ring strain within these metallacyles and upon the presence or absence of Os-bound CH_2 groups, which we find are susceptible to C−H activation by the adjacent Rh center. The Rh/Os combination appears to have the ideal combination of coordinative unsaturation and lability at Rh to promote C−C bond formation, combined with stronger metal−carbon bonds at Os, which serves to keep the hydrocarbyl fragments anchored to this metal during the transformations of interest.

Acknowledgment. We thank the Natural Sciences and Engineering Council of Canada (NSERC) and the University of Alberta for financial support of the research and NSERC for funding for the X-ray diffractometer and the Nicolet FTIR spectrometer.

Supporting Information Available: Tables of X-ray experimental details, atomic coordinates, interatomic distances and angles, anisotropic thermal parameters, and hydrogen parameters for compounds **5**, **6**, **7**, **8**, and **15**. ORTEP diagrams of compounds **6** and **8** are also included. This material is available free of charge via the Internet at http://pubs.acs.org.

OM058041X